

Non-muscle Myosin Contractility in the Neuroblasts Influences Epidermal Morphogenesis

Karina Mastronardi

A
Thesis
in the Department
of
Biology

Presented in Partial Fulfillment of the Requirements
For the Degree of
Master of Science (Biology) at
Concordia University
Montreal, Quebec, Canada

November 2015

©Karina Mastronardi, 2015

CONCORDIA UNIVERSITY
School of Graduate Studies

This is to certify that the thesis prepared

By: Karina Mastronardi
Entitled: Non-muscle Myosin Contractility in the Neuroblasts
Influences Epidermal Morphogenesis

and submitted in partial fulfillment of the requirements for the degree of

Master of Science (Biology)

complies with the regulations of the University and meets the accepted standards with respect to originality and quality.

Signed by the final Examining Committee:

_____	Chair
T.B.A.	
_____	External Examiner
Dr. Catherine Bachewich	
_____	Examiner
Dr. Michael Sacher	
_____	Examiner
Dr. Malcolm Whiteway	
_____	Supervisor
Dr. Alisa Piekny	

Approved by _____
Dr. Selvadurai Dayanandan, Graduate Program Director

_____ 2015 _____
Dean of Faculty

ABSTRACT

Non-muscle Myosin Contractility in the Neuroblasts Influences Epidermal Morphogenesis

Karina Mastronardi

Tissue morphogenesis requires myosin-dependent events such as cell shape changes and migration to be coordinated between cells within a tissue, and/or with cells from other tissues. However, few studies have investigated the simultaneous morphogenesis of multiple tissues *in vivo*. We found that during *C. elegans* ventral enclosure, when epidermal cells collectively migrate to cover the ventral surface of the embryo, the underlying neuroblasts (neuronal precursor cells) also undergo morphogenesis. We found that myosin accumulates as foci along the junction-free edges of the ventral epidermal cells to form a ring, whose closure is myosin-dependent. We also observed the accumulation of myosin foci and the adhesion junction protein α -catenin in the underlying neuroblasts. Our data shows that myosin is required in the neuroblasts for ventral enclosure, and may help to reorganize a subset of neuroblasts into a rosette-like pattern, and decrease their surface area as the overlying epidermal cells constrict. Thus, we propose that mechanical forces in the neuroblasts influence constriction of the overlying epidermal cells. In support of this model, disrupting neuroblast cell division or altering their fate influences myosin localization in the overlying epidermal cells. The coordination of myosin-dependent events and forces between cells in different tissues could be a common theme for coordinating morphogenetic events during metazoan development.

Acknowledgements

Firstly, I would like to thank my supervisor, Dr. Alisa Piekny. It has been a pleasure to work with you over the years and I am immensely grateful to you for giving me the opportunity to learn so much whilst conducting my research. Your support and guidance has been invaluable.

I would also like to thank my committee members, Dr. Michael Sacher, Dr. Malcolm Whiteway and Dr. Catherine Bachewich for their continued time and support.

A very special thank you to Yun Chen and Denise Wernike. Yun, thank you for providing me with a great foundation and for having patience with me in my early days. Denise, I appreciate you sharing with me all the tricks of the trade; your advice and guidance has helped me to become a better researcher.

In addition, I would like to thank my other lab mates. Kevin Larocque, thank you for helping me keep our worms in good shape. Daniel Beaudet, thank you for the continued moral support. Madhav Soowamber, Alexa Mariotti and Dilan Jaunky, thank you for the comedic relief.

Finally, I would like to thank *The Centre for Microscopy and Cellular Imaging* (CMCI) at Concordia University. Melina Jaramillo-Garcia and Chloë van Oostende Triplet, I greatly appreciate all of your help, knowledge and skill. You have saved me many a time.

Dedications

I would like to dedicate this thesis to my parents, Sandy and Tony. I would never have been able to accomplish this without your unwavering and continued support and love. I'm a lucky girl to have the best parents in the world. Thank you for believing in me. I love you.

Contribution of Authors

Figure 10. Denise Wernike and I both contributed to the time-lapse images.

Figure 11. Denise Wernike and I both contributed to the time-lapse images.

Figure 12. Denise Wernike and I both contributed to the time-lapse images.

Figure 13. Denise Wernike and I both contributed to the time-lapse images.

Figure 14. Denise Wernike and I both contributed to the time-lapse images.

Figure 15. Denise Wernike and I both contributed to the time-lapse images.

Figure 16. Denise Wernike and I both contributed to the time-lapse images.

Figure 17. Denise Wernike and I both contributed to the time-lapse images.

Figure 18. Denise Wernike and I both contributed to the time-lapse images.

Figure 19. Denise Wernike and I both contributed to the time-lapse images.

Figure 20. Denise Wernike and I both contributed to the time-lapse images.

Figure 21. Denise Wernike and I both contributed to the model.

Table of Contents

Chapter 1: Introduction.....	1
1.1 Cytoskeletal regulators.....	2
1.1.1. Actin.....	2
1.1.2. Myosin.....	3
1.1.3. Anillin.....	4
1.1.4. Adherens Junctions.....	6
1.2 Tissue Morphogenesis.....	8
1.2.1 Epidermal morphogenesis in <i>C. elegans</i>	8
1.2.1.1 Dorsal intercalation.....	9
1.2.1.2 Ventral enclosure.....	12
1.2.1.3 Elongation.....	16
1.2.2 Drosophila dorsal closure.....	18
1.2.3 Rosette organization and function.....	20
1.3 Summary.....	22
Chapter 2: Materials and Methods.....	24
2.1 Strains and alleles.....	24
2.2 Genetic crosses and RNAi.....	25
2.3 Microscopy.....	25
2.4 Image analysis	26

Chapter 3: Results.....	28
3.1 Non-muscle myosin accumulates as foci in the epidermal cells and neuroblasts during ventral enclosure.....	28
3.2 Non-muscle myosin activity is required for ventral enclosure.....	31
3.3 Neuroblasts in the ventral pocket reorganize during ventral enclosure.....	33
3.4 Neuroblast cell shape, number and organization are important factors for ventral enclosure.....	40
3.5 α -catenin localizes to neuroblast cell boundaries during ventral enclosure.....	46
Chapter 4: Discussion.....	49
Chapter 5: References.....	55

List of Figures

Figure 1. Schematic of anillin's structure.....	5
Figure 2. Schematic of the <i>C. elegans</i> adherens junction.....	8
Figure 3. A schematic overview of the developmental timing of morphogenetic Events during <i>C. elegans</i> embryogenesis.....	10
Figure 4. Dorsal intercalation during <i>C. elegans</i> embryogenesis.....	11
Figure 5. Ventral enclosure during <i>C. elegans</i> embryogenesis.....	13
Figure 6. Schematics show neuroblast bridge formation during <i>C. elegans</i> ventral enclosure.....	16
Figure 7. Elongation during <i>C. elegans</i> embryogenesis.....	17
Figure 8. <i>Drosophila</i> dorsal closure.....	19
Figure 9. Mechanisms of rosette formation.....	21
Figure 10. Non-muscle myosin localizes as networks of foci in epidermal cells and neuroblasts during ventral enclosure.....	29
Figure 11. Myosin foci localize as foci near the ventral surface of the embryo.....	30
Figure 12. Myosin foci appear to coalesce as intercellular networks in the ventral epidermal cells.....	32
Figure 13. Neuroblasts in the pocket form rosettes during ventral enclosure.....	34
Figure 14. Neuroblasts form rosettes in 'late' myosin loss-of-function embryos.....	36
Figure 15. Neuroblasts do not form rosettes in 'early' myosin loss-of-function embryos.....	39
Figure 16. Disrupting neuroblast division alters myosin distribution during ventral enclosure.....	42

Figure 17. Neuroblast fate is important for ventral enclosure.....	44
Figure 18. Altering neuroblast fate influences myosin localization during ventral enclosure.....	45
Figure 19. The adherens junction protein α -catenin accumulates in re-organizing neuroblasts during ventral enclosure.....	47
Figure 20. Neuroblasts form disorganized rosettes after mild disruption of <i>hmr-1</i> /E-cadherin function.....	48
Figure 21. Model for myosin regulation and neuroblast organization during ventral enclosure.....	50
Figure 22. Pathway for myosin regulation and neuroblast organization during ventral enclosure.....	51

Chapter 1: Introduction

This thesis will elucidate the role of mechanical forces in tissue morphogenesis. Using *C. elegans* as a model organism, we describe how multiple tissues undergo morphogenesis concomitantly, and how one tissue may influence the other. *C. elegans* offers several advantages as a model organism because it is amenable to genetic studies, has a short life span and large brood size, and has the ability to self fertilize as hermaphrodites or be outcrossed to males. Additionally, it is well suited for transgenics, RNAi and microscopy, and previous studies have revealed the precise order and timing of events during embryonic development. Furthermore, its simplicity permits us to study intercellular signaling between cells of the same tissue as well as between cells of different tissues.

In particular, our *in vivo* studies describe neuroblast and epidermal morphogenesis, which occurs during mid-late embryogenesis. For the first time, we show how a subset of neuroblasts undergo cell shape changes and rearrangements during morphogenesis of the overlying epidermis. These neuroblasts form a circular pattern (very similar to a rosette) which decreases in surface area and may draw in the overlying epidermal cells closer together to encase the embryo in a layer of epidermis.

First, I will describe the different cytoskeletal components and regulators that are important for morphogenesis, as well as adhesion junctions that translate cytoskeletal forces into cell shape changes and movements. Next, I will describe morphogenetic events important for development, with an emphasis on *C. elegans* epidermal morphogenesis.

1.1 Cytoskeletal Regulators

1.1.1 Actin

Two types of F-actin are essential for *C. elegans* epidermal morphogenesis: short, branched filaments mediate migration, while long, un-branched filaments associated with non-muscle myosin provide contractility for cell shape changes (Chisholm and Hardin 2005; Williams-Masson, 1997). The branching of actin filaments is achieved by the activity of Arp2/3, a seven-subunit protein that mimics the core actin complex required to nucleate F-actin (a G-actin trimer), and templates the growth of F-actin from pre-existing filaments at a 70° angle (Pollard et al., 2000; Amann and Pollard, 2001; Goley and Welch, 2006). Arp2 and Arp3, however, possess little activity on their own and require activation by the WASp (Wiskott-Aldrich syndrome protein) and WAVE/SCAR (WASp family verprolin homology proteins/suppressor of cAMP receptor) complexes, which bind to the Arp2/3 complex to promote actin nucleation. Mutations in GEX-2 or GEX-3, which are components of the WAVE/SCAR complex in *C. elegans*, cause ventral enclosure phenotypes where the ventral epidermal cells fail to migrate and remain on the dorsal surface of the embryo causing the internal contents to extrude (see Chapter 1.2.1.2). In particular, *gex-2/3* mutants have disorganized F-actin and subsets of epidermal cells cannot make the filopodial/lamellipodial projections required for their migration (Patel et al., 2008).

Long, unbranched F-actin is nucleated and polymerized with the help of profilins and formins, but many of the genes regulating this type of F-actin have not been studied in *C. elegans* mid-late embryogenesis due to their requirement in the early embryo for cytokinesis. One gene, *fhod-1*, is a formin that was recently shown to regulate the formation of microfilaments that associate with active myosin in a subset of epidermal cells to drive

elongation of the embryo from an ovoid into the vermiform larva (see Chapter 1.2.1.3; Vanneste et al., 2013).

1.1.2 Myosin

The formation and activation of non-muscle myosin filaments is essential for cell shape changes, and likely other cellular events required for morphogenesis. Non-muscle myosin II binds to F-actin and generates tensile force by sliding neighbouring actin filaments past one another, or by acting as a crosslinker. Non-muscle myosin II is comprised of a pair of heavy chains, a pair of regulatory light chains (RLC) and a pair of essential light chains (ELC). Each heavy chain possesses a catalytic motor head domain in its N-terminus, which has highly conserved actin-binding and ATP-binding sites. Both the RLC and ELC associate with the neck region of the heavy chain, which lies adjacent to the motor (Vincente-Manzanares et al., 2009). Non-muscle myosin activity is regulated by phosphorylation of the RLC, which promotes dimerization of the heavy chains and stimulates ATPase activity in the motor (Vincente-Manzanares et al., 2009). There are several kinases known to phosphorylate the RLC at conserved Thr18 and/or Ser19 residues, including Rho kinase, citron kinase and myosin light chain kinase (Yamashiro et al., 2003; Matsumura, 2005; Vincente-Manzanares et al., 2009). Conversely, myosin phosphatase removes these phosphates to render myosin inactive (Yamashiro et al., 2003, Vincente-Manzanares et al., 2009). Interestingly, Rho kinase can phosphorylate and inactivate the regulatory subunit of myosin phosphatase causing an increase in myosin contractility (Vincente-Manzanares et al., 2009).

Myosin's function during *C. elegans* epidermal elongation (see Chapter 1.2.1.3) has been well characterized. The process of elongation allows for the ovoid embryo to stretch out into the classic vermiform shape of the adult worm and is driven by cell shape changes in a subset of

epidermal cells called the seam cells (lateral hypodermal cells; Chisholm and Hardin, 2005). Two heavy chain paralogues, NMY-1 and NMY-2, as well as the essential light chain, MLC-3, and the regulatory light chain, MLC-4, are all required to mediate the seam cell shape changes required for elongation (Shelton et al., 1999; Piekny et al., 2003; Gally et al., 2009). Furthermore, as described above, the loss of Rho kinase (LET-502) prevents the lateral epidermal cells from changing shape, whereas loss of myosin phosphatase regulatory subunit (MEL-11) causes the seam cells to hyperconstrict, causing the embryos to rupture (Wissmann et al., 1997). We found that myosin and its regulators are also required for ventral enclosure (Fotopoulos et al. 2013; Wernike et al., 2015 in revision). However, it is not clear how myosin contractility is spatially controlled at this time, and what cellular events it helps to mediate.

1.1.3 Anillin

Our lab recently found that the actin-myosin binding protein ANI-1 (anillin) is required for ventral enclosure, part of *C. elegans* epidermal morphogenesis (see Chapter 1.2.1.2), by controlling neuroblast cell division (Fotopoulos et al., 2013). Anillin is a highly conserved protein that interacts with multiple proteins for cytokinesis, an event that occurs at the end of mitosis to separate the daughter cells. This process occurs due to the formation and ingression of a discrete actin-myosin contractile ring. Active RhoA recruits anillin to the equatorial cortex during cytokinesis, where anillin binds to actin and myosin in the contractile ring and stabilizes it during ingression (Piekny and Maddox, 2010). There are three distinct anillin isoforms in *C. elegans*: *ani-1*, which shares the highest homology with both human and *Drosophila* anillin, and *ani-2* and *ani-3*, which encode truncated forms that lack the characteristic actin and myosin binding sites (Figure 1; Maddox et al., 2005). There is no known function for *ani-3*, however

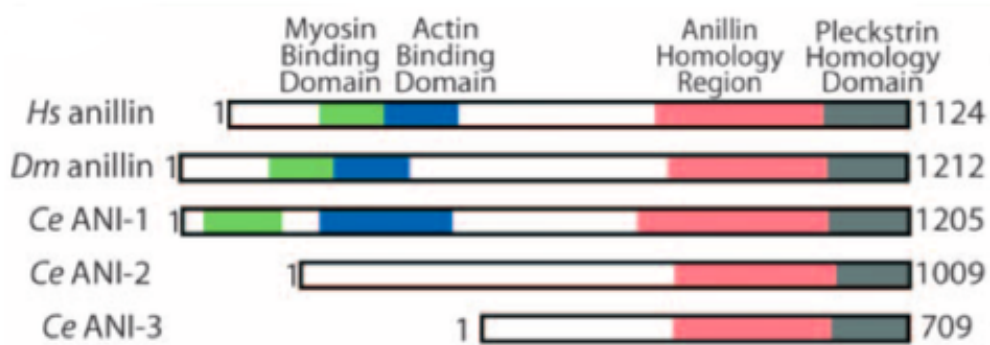


Figure 1. Schematic of anillin’s structure. Cartoon schematics show human, *Drosophila* (*scraps*) and *C. elegans* (isoforms ANI-1, ANI-2 and ANI-3) anillin homologues. The myosin binding domain is green, the actin binding domain is blue, the Anillin Homology region (containing binding sites for RhoA and phospholipids) is in pink and the Pleckstrin Homology domain is in grey. ANI-1 shares highest homology with anillins from other metazoans, while ANI-2 and ANI-3 lack the N-terminal binding domains. This figure is adapted from Maddox et al. (2005).

ani-2 is required for germline development (Maddox et al., 2005, Amini et al., 2014). In the early embryo, *ani-1* depletion results in abnormal constriction of the contractile ring, although cytokinesis still succeeds (Maddox et al., 2007). As mentioned above, our lab found that *ani-1* is primarily expressed in the neuroblasts and is required for neuroblast cytokinesis, which gives rise to ventral enclosure phenotypes (Fotopoulos et al., 2013). Ventral enclosure is the stage in epidermal morphogenesis whereby the ventral epidermal cells migrate over the embryo, using cues from the underlying neuroblasts, to meet at the ventral midline in order for the embryo to become encased in a layer of epidermis. In *ani-1*-depleted embryos, neuroblasts are misshapen and are often multinucleate. This may prevent the ventral epidermal cells from migrating properly, as we found that they were misaligned and the embryos were prone to rupture during elongation (Fotopoulos et al., 2013). Interestingly, we also found that *ani-1* lethality is partially suppressed by over-expressing α -catenin (a component of adherens junctions as described in 1.1.4). Since α -catenin tethers to intracellular F-actin, ANI-1 could also be required to tether F-actin to generate tension in the neuroblasts for ventral enclosure (Fotopoulos et al., 2013).

1.1.4 Adherens Junctions

Cells are coordinated for the morphogenesis and maintenance of tissues via adhesion junctions. These junctions have extracellular proteins that permit neighbouring cells to adhere, and intracellular proteins that tether to actomyosin networks. Thus, forces can be transmitted across multiple cells to allow them to behave as a cohesive unit (Harris and Tepass, 2010). *C. elegans* epidermal cells are connected via sub-apical adherens junctions that are comprised of at least two partially redundant complexes; the catenin-cadherin complex (CCC) and the DLG-

1/AJM-1 complex (DAC) (Figure 2; Labouesse, 2006). The CCC is a multi-subunit complex containing E-cadherin (HMR-1), α -catenin (HMP-1) and β -catenin (HMP-2) (Costa et al., 1998; Labouesse, 2006). HMR-1 is a transmembrane protein with both extra- and intracellular domains. The extracellular domain homodimerizes with HMR-1 on an adjacent cell, while the intracellular domain forms a complex with F-actin, HMP-1 and HMP-2 (Costa et al., 1998; Labouesse, 2006). Throughout embryogenesis, most cells are connected via junctions containing CCC's and mutations in the CCC do not cause tissues to fall apart, suggesting that redundant complexes can function in their absence. However, mutations cause abnormal body morphologies during late embryogenesis. It was proposed that these phenotypes arise due to problems with the assembly of de novo junctions, causing decreased junction integrity between contralateral ventral epidermal cells and the uneven transmission of myosin contractility as epidermal cells elongate (Costa et al., 1998; Chisholm and Hardin, 2005; Labouesse, 2006). Another possibility is that the DAC functionally replaces the CCC in the epidermal cells, but not in the neuroblasts, and the phenotypes arising from disrupted CCC is because of their requirement in the neuroblasts.

1.2 Tissue morphogenesis

1.2.1 Epidermal morphogenesis in *C. elegans* embryos

The morphogenesis of tissues is essential for the development of all metazoans and relies on the coordination of cellular events such as shape changes, migration and adhesion. These events are tightly regulated in response to both chemical and/or mechanical cues coming from neighbouring cells within the tissue, or from other tissues. Misregulation of these processes can cause developmental defects and promote the metastasis of cancer cells, when cells no longer

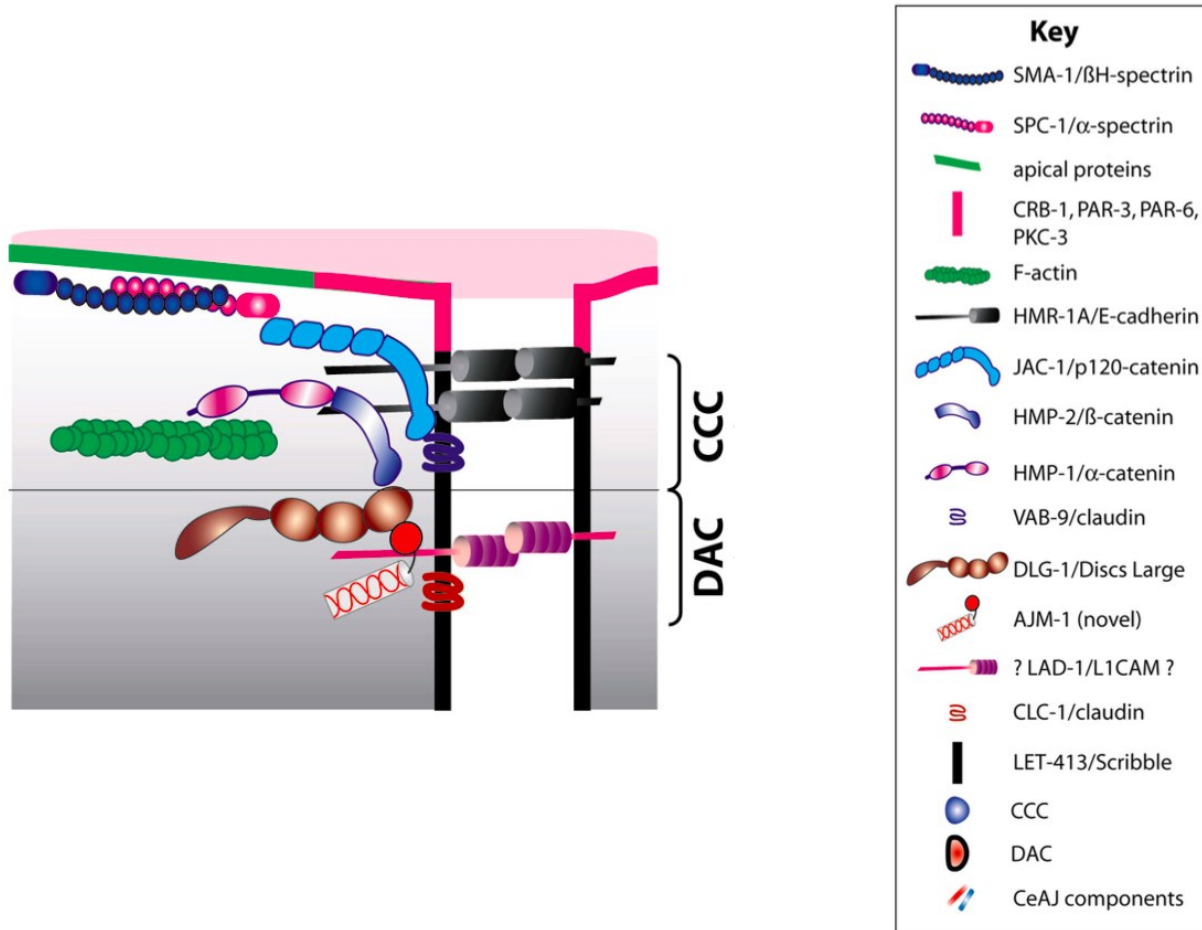


Figure 2. Schematic of the *C. elegans* adherens junction. A cartoon schematic shows the general architecture of adhesion junctions in *C. elegans* epidermal cells. The CCC consists of E-cadherin/HMR-1 (black) that homotypically binds to HMR-1 on adjacent cells via its extracellular domain. Intracellularly, HMR-1 binds to a complex of α -catenin/HMP-1 (pink) and β -catenin/HMP-2 (dark blue), which associates with F-actin (green) and helps tether the cytoskeleton to the junction. The DAC consists of DLG-1/Discs Large (brown) and AJM-1 (novel protein) and tethers to adjacent cells via a transmembrane protein with an extracellular domain, possibly LAD-1/L1CAM (purple). Other proteins are also found in the junction as indicated in the figure legend. This figure is adapted from Labouesse (2006).

respect their tissue boundaries. Therefore, understanding the formation and maintenance of these regulatory processes is extremely important.

We study epidermal morphogenesis in *C. elegans* to understand conserved mechanisms guiding tissue morphogenesis in metazoans. In addition to the benefits *C. elegans* offers as a model organism (see Chapter 1), its simplicity permits us to study intercellular signaling between cells of the same tissue as well as between cells of different tissues.

The *C. elegans* embryo becomes covered in a layer of epidermis and changes shape from a ball into the vermiform, elongated shape of a worm during mid-to-late embryogenesis. Epidermal morphogenesis occurs in three distinct steps: dorsal intercalation, ventral enclosure and elongation. All steps are crucial for embryonic development and I study ventral enclosure, when the ventral epidermal cells migrate to cover the belly of the embryo (Figure 3).

1.2.1.1 Dorsal Intercalation

At the end of gastrulation and around 290 minutes after the first cell division, the epidermal cells are born on the dorsal surface of the embryo. The epidermal cells assemble into six rows and through an event called dorsal intercalation, the cells in the inner two rows interdigitate to form a single row of cells. During this process, the dorsal epidermal cells start off as round-shaped and become wedge-shaped as they push between their contralateral neighbours. The cells subsequently become rectangular in shape, which results in a flat sheet of twenty cells on the dorsal side of the embryo (Figure 4). The mechanism that drives this process was recently shown to involve regulation of actin-mediated protrusions for cell movements, which are controlled by Rac and RhoG small GTPases (Walck-Shannon et al. 2015). They function upstream of complexes including WAVE/Scar and WASP that regulate the formation of short,

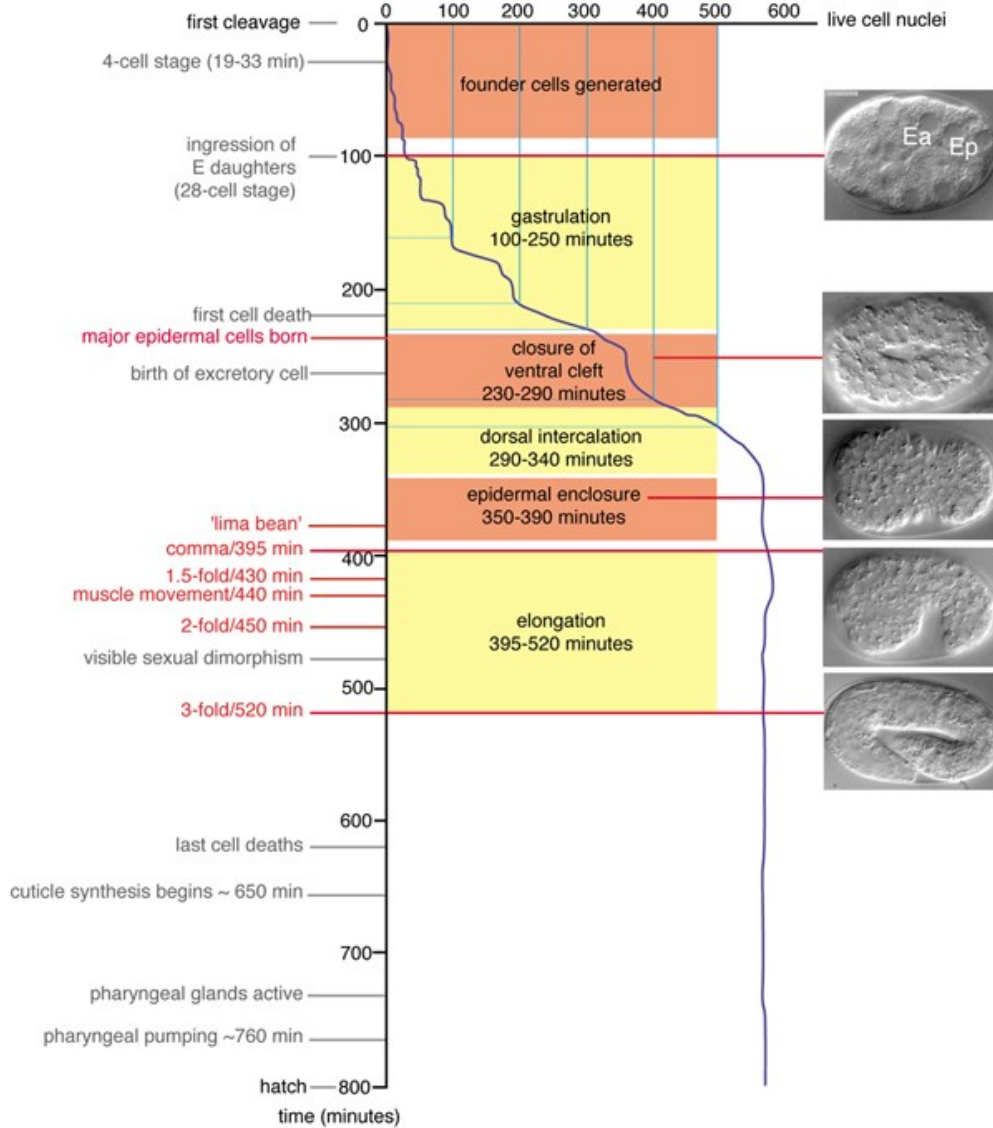


Figure 3. A schematic overview of the developmental timing of morphogenetic events during *C. elegans* embryogenesis. A graph shows the number of cells (X-axis - live nuclei) in the embryo over time (Y-axis – in minutes) from fertilization. Hallmark stages of embryonic development are indicated on the Y-axis. Morphogenetic events including gastrulation, cleft closure and epidermal morphogenesis are highlighted in the coloured boxes. To the right are Differential Interference Contrast (DIC) microscopy images of embryos at the corresponding stages as indicated by the red lines. Epidermal morphogenesis occurs between ~290-520 minutes after the first cell division and includes dorsal intercalation, ventral enclosure and elongation. The scale bar is 5 μ m. This figure is adapted from Chisholm and Hardin (2005).

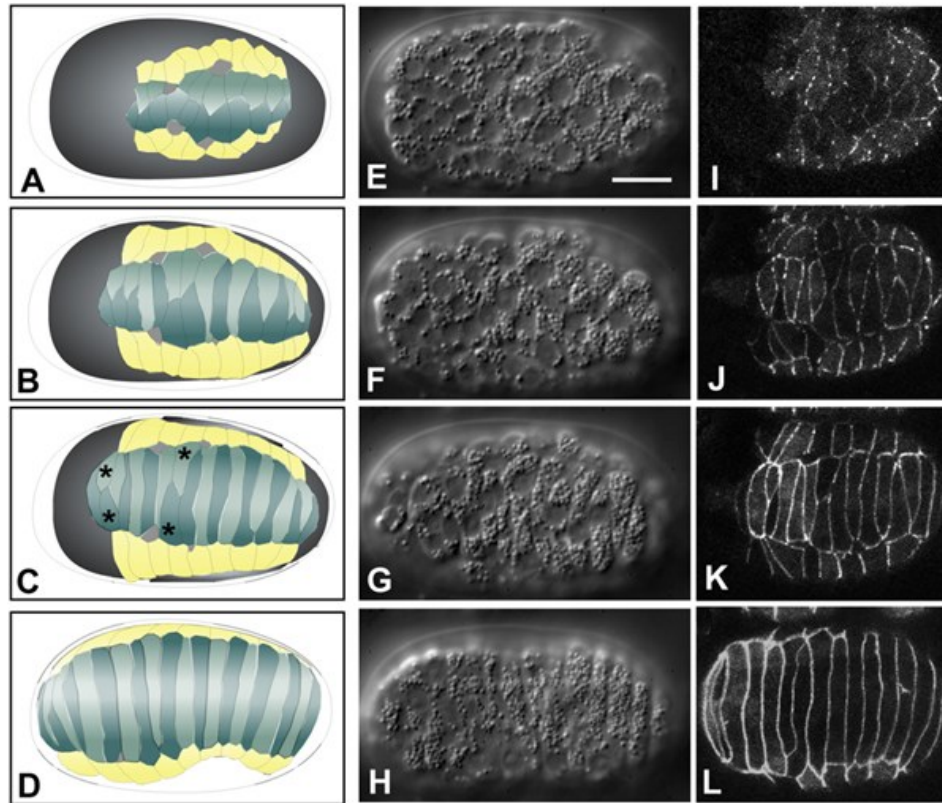


Figure 4. Dorsal intercalation during *C. elegans* embryogenesis. The left column shows cartoon schematics of the different stages of dorsal intercalation, while the middle column shows DIC images of embryos at these stages and the right column depicts DLG-1:GFP (epidermal adherens junction marker) fluorescence micrographs. The dorsal cells are light and dark green and the seam cells (lateral epidermal cells) are yellow. At the onset of dorsal intercalation, the dorsal cells become wedge-shaped and interdigitate between their partners on the opposite side of the dorsal midline (top two rows). As they intercalate, the dorsal epidermal cells also elongate until they establish contacts and form adhesion junctions with the lateral seam cells (third row). A complete dorsal sheet is established once all of the dorsal cells have fully elongated (bottom row). The scale bar is 5 μm . This figure is adapted from Chisholm and Hardin (2005).

branched F-actin via Arp 2/3 (Walck-Shannon et al. 2015). We have also seen the accumulation of another Rho GTPase, the RhoA homologue, at the edges of the cells that become wedge-shaped (Fotopoulos et al. 2013). Since RhoA regulates actin-myosin contractility, this also may be an important mechanism controlling cell shape changes for dorsal intercalation.

1.2.1.2 Ventral Enclosure

Ventral enclosure occurs after dorsal intercalation to cover the belly or ventral surface of the embryo in a layer of epidermis. The ventral epidermal cells collectively migrate towards the ventral midline where they adhere to their contralateral partners. Ventral enclosure occurs in two distinct stages. First, two pairs of anterior epidermal, or leading edge, cells migrate toward the ventral midline by filipodial/lamellipodial projections that are rich in short, branched F-actin (Figure 5). Inactivating these cells by ablation or inhibiting F-actin polymerization disrupts ventral enclosure by either slowing down or completely halting migration (Williams-Masson et al., 1997). As with dorsal intercalation, Rac regulates the formation of F-actin-rich protrusions via WAVE/Scar or WASP and the Arp 2/3 complex (Soto et al., 2002; Patel et al., 2008). Embryos with mutations in the *gex-2/gex-3* genes that encode components of the WAVE/SCAR complex have defective ventral epidermal cell migration and display GEX (gut on the exterior) phenotypes, where the internal contents of the embryo are extruded (Soto et al., 2002; Patel et al., 2008). The effect that these mutations have on the ability of ventral epidermal cells to migrate underlines the significance of regulating F-actin for cell migration during ventral enclosure. During the second stage of ventral enclosure, the posterior ventral epidermal (pocket) cells become wedge-shaped and form a ring that then constricts closed over the ventral surface of the embryo (Figure 5; Chisholm and Hardin, 2005; Zhang et al., 2010). Long F-actin cables

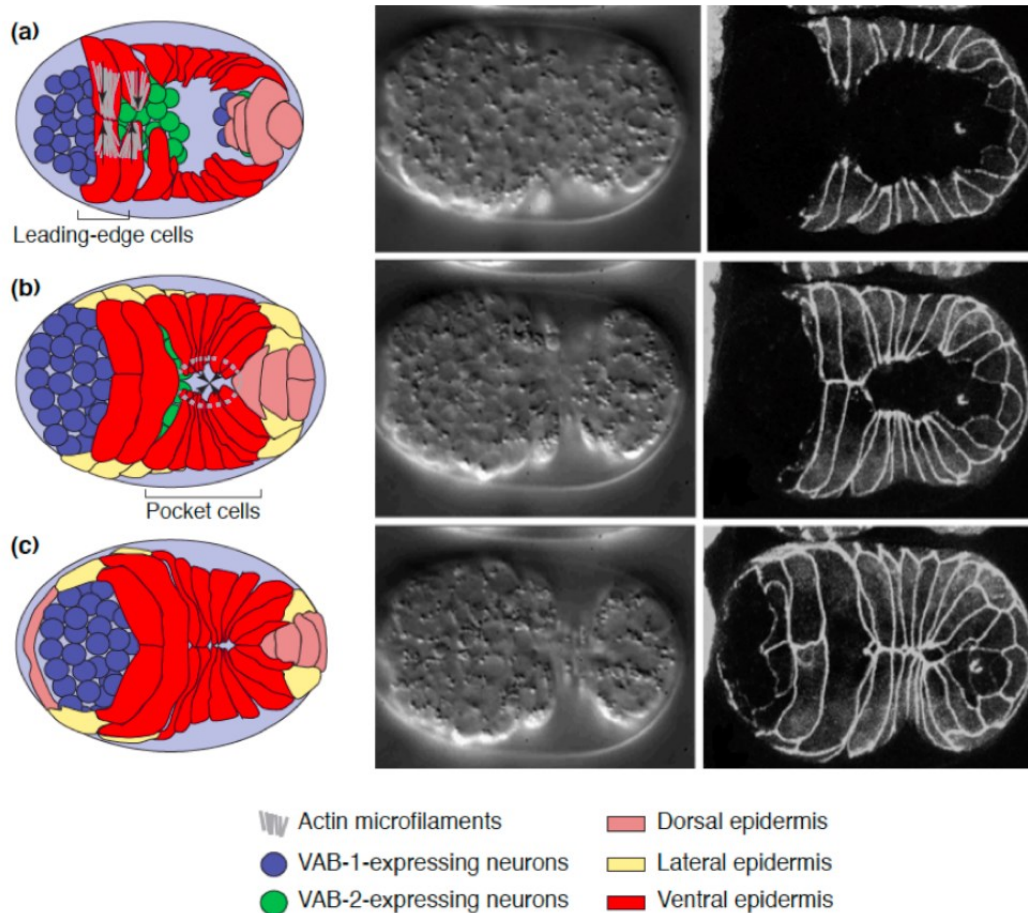


Figure 5. Ventral enclosure during *C. elegans* embryogenesis. The left column shows cartoon schematics of an embryo going through ventral enclosure, while the middle column shows corresponding DIC images and the right column depicts DLG-1:GFP (epidermal adherens junction marker) fluorescence micrographs. The ventral epidermal cells are red, the seam cells are yellow and the dorsal cells are pink. The blue and green cells are different subsets of underlying neuronal precursor cells (neuroblasts). In (a) two pairs of leading-edge cells migrate toward the ventral midline using actin-rich protrusions (grey lines). In (b), the posterior-positioned pocket epidermal cells form a ring that constricts closed over the embryo. In (c), contralateral ventral epidermal cells adhere at the ventral midline. This figure is adapted from Chin-Sang and Chisholm (2000) and Chisholm and Hardin (2005).

accumulate along the junction-free edge of the pocket epidermal cells, thereby forming an actin ring around the ventral pocket (Williams-Masson et al., 1997). We recently showed that myosin contractility likely constricts this ring, although we still do not know how it is regulated (Fotopoulos et al. 2013; Wernike et al. 2015 in revision).

Successful ventral enclosure requires cues from the underlying neuroblasts (neuronal precursor cells). The neuroblasts may provide chemical cues that mediate ventral epidermal cell migration. For example, the VAB-2/EFN-1 ligand is expressed in a subset of neuroblasts and could signal to VAB-1 receptor in the epidermal cells. Interestingly, another subset of neuroblasts express the VAB-1 receptor, where it is required to sort them into distinct locations from the EFN-1-expressing cells (Chin-Sang et al., 1999; Chin-Sang et al., 2002). This results in an enrichment of EFN-1 expressing cells in the middle of the embryo (Chin-Sang et al., 1999; Chin-Sang et al., 2002). However, VAB-1 is also required in the ventral epidermal cells to help mediate their migration, by controlling the direction and formation of F-actin projections (Patel et al., 2008; Bernadskaya et al., 2012). Therefore, it is not clear if the sole function of the neuroblasts in ventral enclosure is to provide the epidermal cells with tethered EFN-1 ligand. Other receptors are also required in the epidermal cells to control their migration for ventral enclosure, including UNC-40 (DCC – netrin receptor) and SAX-3/Robo (SLIT receptor) (Bernadskaya et al., 2012). It is not clear how these pathways function together for ventral enclosure, and if the ligands are expressed/required in the neuroblasts or in neighbouring epidermal cells. Another study showed that a subset of pocket epidermal cells relies on the formation of a neuroblast bridge to migrate successfully (Ikegami et al., 2012). Previously known for its function in axon guidance, semaphorin/plexin signaling also regulates ventral enclosure (Roy et al., 2000). Five pairs of neuroblasts expressing PLX-2, a semaphorin receptor,

arrange themselves with bilateral symmetry in order to direct pocket cell migration toward the ventral midline during ventral enclosure (Figure 6; Ikegami et al., 2012). Interestingly, these neuroblasts make protrusions towards their neighbouring cells, which overlap and help to maintain cohesion via this “bridge” (Ikegami et al., 2012). This data suggests that neuroblast positioning is important for successful ventral enclosure, but it is not clear if this positioning is because they provide tethered ligands to the epidermal cells or because they also provide mechanical cues.

1.2.1.3 Elongation

After ventral enclosure embryos undergo elongation, the last stage in epidermal morphogenesis, where embryos form their characteristic vermiform shape (Chisholm and Hardin, 2005). Elongation primarily occurs by myosin-mediated contraction of highly organized actin filaments within the seam cells (lateral epidermal cells). The forces generated by myosin cause these cells to squeeze from cuboidal to cylindrical in shape along the anterior-posterior axis (Priess and Hirsch, 1986). To generate sufficient active myosin to drive contractility within the seam cells, a positive regulator of myosin contractility, LET-502 (Rho kinase) is highly expressed in the seam cells, while a negative regulator of myosin contractility, MEL-11 (myosin phosphatase regulatory subunit) is highly expressed in the dorsal and ventral epidermal cells (Figure 7; Chin-Sang and Chisholm, 2000). Based on studies done in other organisms, LET-502 (Rho kinase) likely phosphorylates MLC-4 (non-muscle regulatory light chain) to form active myosin filaments (Amano et al., 1996; Ishizaki et al., 1996). Loss-of-function mutations in *let-502* prevents the seam cells from changing shape and impairs elongation, likely due to insufficient levels of active myosin (Piekny et al., 2000). The MEL-11 homologue (myosin

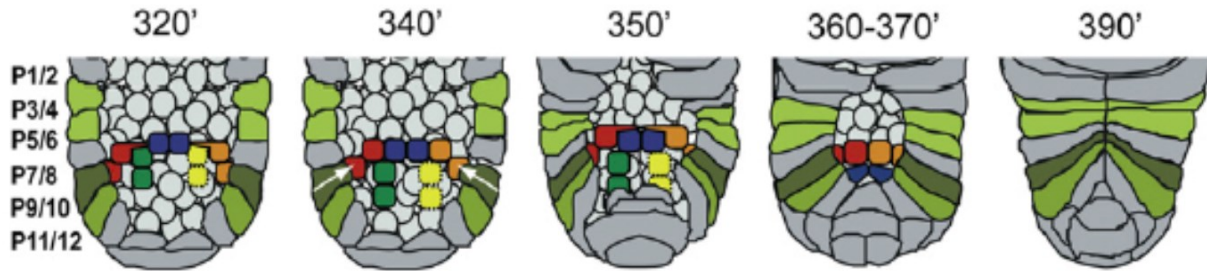


Figure 6. Schematics show neuroblast bridge formation during *C. elegans* ventral enclosure. Cartoon schematics show the different stages of pocket closure as indicated in minutes after first cell division. Five pairs of PLX-2-expressing neuroblasts (red, green, blue, yellow and orange) span across the open ventral pocket to form a bridge. Plexin-bands of cells of the same color are sisters (daughters from the preceding cell division). Laterally oriented sisters on either side of the embryo (red and orange) form protrusions (at 320 and 350 minutes) that overlap with neighboring cells (in blue). The neuroblast bridge enables the overlying epidermal pocket cells (P9/10) to migrate toward the ventral midline. This figure is adapted from Ikegami et al. (2012).

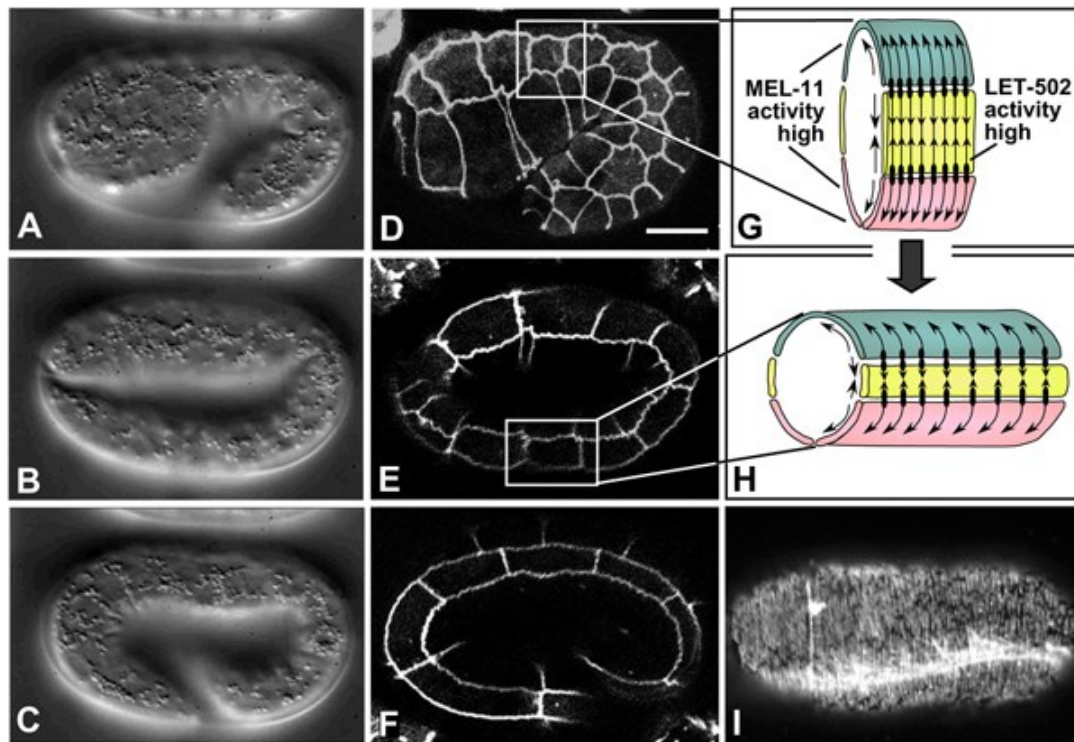


Figure 7. Elongation during *C. elegans* embryogenesis. The left column shows DIC images of embryos during the different stages of elongation, while the middle column depicts DLG-1:GFP (epidermal adherens junction marker) fluorescence micrographs and the right column shows cartoon schematics for each stage. In the schematics, the ventral epidermal cells are pink, the seam cells are yellow and the dorsal cells are green. High levels of LET-502/Rho kinase lead to an increase in the levels of active myosin in the seam cells to promote drastic changes in their shape along the anterior-posterior axis. In contrast, MEL-11/myosin phosphatase is highly expressed in the dorsal and ventral epidermal cells, causing a decrease in myosin activity in these cells. The scale bar is 5 μ m. This figure is adapted from Chisholm and Hardin (2005).

phosphatase regulatory subunit) likely promotes relaxation by dephosphorylating myosin and returning it to its inactive state. Loss-of-function mutations in *mel-11* cause the seam cells to hyperconstrict, likely due to uncontrolled myosin activity (Wissmann et al., 1997; Wissmann et al., 1999). Interestingly, the balance of myosin regulation is important for elongation to occur properly, since *let-502* and *mell-11* mutants suppress one another, causing embryos to elongate normally (Wissmann et al., 1997; Piekny et al., 2000).

1.2.2. Drosophila Dorsal Closure

In an analogous process in *Drosophila* called dorsal closure, where the dorsal epidermal cells cover the dorsal part of the embryo, the underlying amnioserosal cells provide mechanical inputs to the overlying epithelial cells (Kiehart et al., 2000). In these amnioserosal cells, myosin contractility causes them to constrict apically, which decreases their surface area and helps pull the overlying epidermal cells closer together (Figure 8; Solon et al., 2009). In addition, actin-myosin filaments assemble at the dorsal edge of the dorsal-most row of epidermal cells, which close via a purse-string mechanism (Kiehart et al., 2000). We found that myosin contractility is required for successful ventral enclosure (Fotopoulos et al., 2013; Wernike et al., 2015 in revision). Mechanical forces constrict the pocket epidermal cells to close over the ventral surface, and myosin could be required in the neuroblasts to regulate their movements and/or cell shape changes (Fotopoulos et al., 2013; Wernike et al., 2015 in revision). Although ventral enclosure and dorsal closure may share some analogies, there is one key difference. The amnioserosal cells are epithelial and are tethered to each other via adhesion junctions and changes in their shape are coordinated across the tissue. However, the neuroblasts are neuronal precursor cells that lack epidermal markers and while at least some of these cells likely form

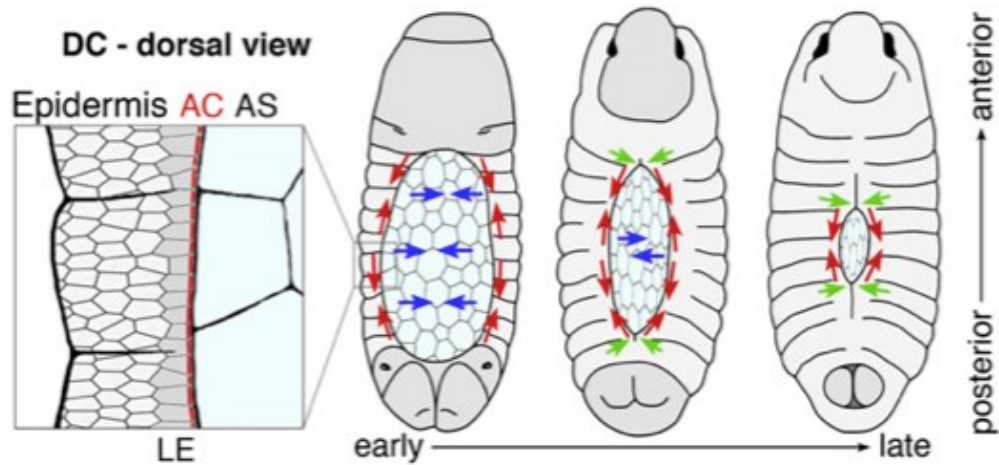


Figure 8. *Drosophila* dorsal closure. Cartoon schematics show a *Drosophila* embryo during dorsal closure. The zoomed in region (box on the left) depicts the leading edge (LE) of the epidermis (left) with the actin cable (AC) and the adjacent amnioserosal cells (right). The coloured arrows show the direction of movements and forces produced by the AS cells (blue), the AC (red), and zippering (green) of the epidermal cells. Figure adapted from Solon et al., 2009.

junctions, they have not been extensively studied at this stage of development.

1.2.3 Rosette Organization and Function

Part of tissue morphogenesis involves the reorganization of cells within the tissue to promote its extension in a different plane or to help cells become differently organized vs. others (Lecuit and Lenne, 2007). Multicellular rosettes, when multiple cells share a common vertex, have been described as important intermediates for re-organizing cells in developing tissues (Figure 9). One mechanism that drives rosette formation and resolution utilizes apical constriction, while the other describes those that form through planar polarity, which I will not discuss. The formation of rosettes via apical constriction is best described in epithelial tissue, and occurs via coordinated actin-myosin contractility to simultaneously constrict the apical regions of multiple cells (Lecuit and Lenne, 2007; Harding et al., 2014). As this occurs, the adhesion junctions shrink and subsequently reform with new neighbours as the rosette resolves (Blankenship et al., 2006). While rosettes have not been described yet for *C. elegans* epidermal morphogenesis, one study proposed that as the pocket ventral epidermal cells constrict to close over the ventral surface of the embryo, their coordinated constriction may occur via a rosette-like mechanism (Roh-Johnson et al., 2012). However, we have evidence that subsets of neuroblasts form myosin-dependent rosettes, which may be crucial to help elongate the tissue in preparation for epidermal elongation (Wernike et al., 2015 in revision). Alternatively, the rosettes may help coordinate myosin contractility to generate tension that is sensed by the overlying epidermal cells to coordinate their migration/movement toward the ventral midline (Wernike et al., 2015 in revision).

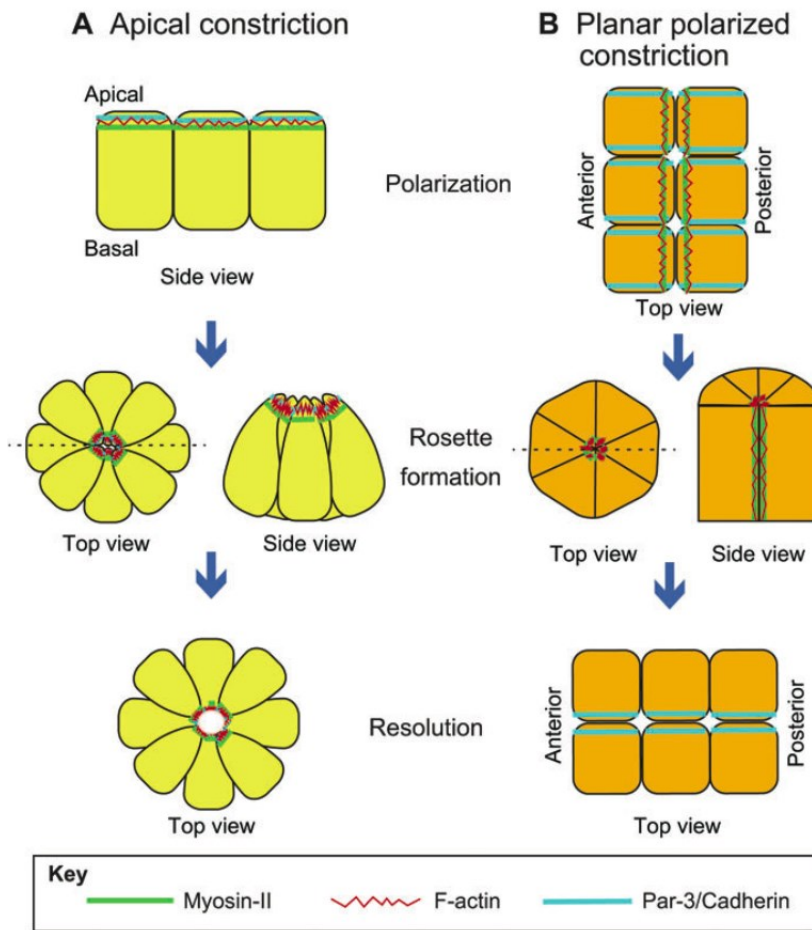


Figure 9. Mechanisms of rosette formation. (A) Rosette formation via apical constriction. Apical constriction leads to the formation of a rosette around an actin-myosin-rich center. Note that only apical, but not basal, domains of rosette cells are constricted. Following rosette formation, rosette centers may open to form a central lumen. (B) During rosette formation via planar polarized constriction, cytoskeletal molecules are distributed in a planar polarized fashion throughout the developing tissue prior to rosette formation. Rosettes formed in this manner often resolve along the axis perpendicular to that of the initial cellular arrangement. Dashed lines indicate the plane of the cross-sections shown. Myosin is green, F-actin is red and Par-3/Cadherin is blue. This figure is adapted from Harding et al. (2014).

1.3 Summary

We found that myosin is required in the neuroblasts for ventral enclosure. Myosin accumulates as foci along the junction-free edges of the epidermal cells surrounding the ventral pocket, where it may generate force on F-actin to constrict the pocket. Interestingly, myosin also accumulates as foci in the underlying neuroblasts. Myosin contractility is required for ventral enclosure because mutations in either myosin, or one of its upstream regulators, caused ventral enclosure phenotypes. Importantly, we found that myosin is required specifically in the neuroblasts, supporting the model that the neuroblasts provide mechanical forces to influence the overlying epidermal cells. We also found that a subset of neuroblasts in the ventral pocket organizes into a rosette-like pattern, and their surface area decreases as the overlying epidermal cells constrict the ventral pocket. Their change in surface area could help bring the overlying epidermal cells closer together. An alternative, and not mutually exclusive model, is that the neuroblasts undergo rearrangements to prepare the tissue for epidermal elongation. And as the cells form these different arrangements, they may generate tension that is sensed by the overlying epidermal cells.

In support of a crucial, mechanical role for neuroblasts in ventral enclosure, we found that α -catenin is also expressed in the neuroblasts and localizes to cell boundaries with a pattern highly reminiscent of myosin. We propose that CCC junctions form between neuroblasts and may help to anchor actin-myosin filaments to transmit forces across the cells. This may occur for rosette formation and resolution and/or to generate tension that is sensed by the overlying epidermal cells. In support of either model, the *ani-1* RNAi phenotype is suppressed by the over-expression of the CCC component HMP-1, and *ani-1* RNAi enhances loss of *hmp-1*, *hmp-2* or *hmr-1*. This suggests that ANI-1 could potentially crosslink actin filaments at junctions in the

neuroblasts, which is important to generate tension for either rosette formation or for mediating epidermal cell migration. In support of the latter model, disrupting neuroblast cell division via *ani-1* RNAi causes myosin to be asymmetrically accumulated in the overlying epidermal cells.

Chapter 2: Materials and Methods

2.1 Strains and alleles

C. elegans stocks were maintained on NGM plates with *E. coli* (OP-50) according to standard protocols (Brenner, 1974). The following strains were obtained from the *Caenorhabditis* Genetics Center (CGC): N2 (wild-type), *nmy-2 (ne1490) I*, *ect-2 (ax751) II*, *mlec-4 (or253)/qC1 dpy-19 (e1259) glp-1 (q339) III*, *unc-119 (ed3) III*; *tjls1 [pie-1::GFP::rho-1 + unc-119(+)]*, *ajm-1 (ok160) X*; *jcEx44, rho-1 (ok2418)/nT1 [qIs51] I*, *mcls46 [dlg-1::RFP + unc-119]*, *ltIs44pAA173 [pie-1p-mCherry::PH(PLC1delta1) + unc-119(+)]*, *lin-15B (n744)*; *uls57 [unc-119p::YFP + unc-119p::sid-1 + mec6p::mec6]*, *hmp-1(zu278)/daf-11(m84) sma-1(e30) V*, *hmp-2(qm39) I*, *hmp-2(zu364)/hIn 1 [unc-54(h1040)] I*, *unc-3(e151) X*, *hlh-14(gm34)/mnC1 dpy-10(e128) unc-52(e444) II*] and *hmr-1(zu389)/dpy-5(e61) I*. The following strains were obtained from colleagues: *let-502 (sb118)* from P. Mains (U. Calgary), *unc-4 (e120) ect-2 (zh8) II* from A. Hajnal (U. Zurich), *ect-2 (gk44) II*; *unc-119 (ed3) III*; *xnIs162 [ect-2::GFP + unc-119(+)]* from J. Nance (Skirball Institute), *nmy-2 (cp7 [nmy-2::gfp + LoxP unc-119(+)] LoxP) I* from B. Goldstein (UNC), and *pRI.20 Pplx-2::GFP* (transcriptional reporter) from J. Culotti (U. Toronto). The following strains were made for this study: *nmy-2 (ne1490)*; *AJM-1:GFP, let-502 (sb118)*; *AJM-1:GFP, let-502 (sb118)*; *ect-2 (ax751)*; *AJM-1:GFP, ect-2 (ax751)*; *AJM-1:GFP, ect-2 (zh8)*; *AJM-1:GFP, ect-2 (ax751)*; *rho-1 (ok2418)/+*, *ect-2 (ax751)*; *mlec-4 (or253)/+*, *let-502 (sb118)*; *ect-2 (ax751)*, *NMY-2:GFP*; *ect-2 (ax751)*, *NMY-2:GFP*; *ect-2 (zh8)*, *ect-2 (zh8)*; *rho-1 (ok2418)/+*, *NMY-2:GFP*; *DLG-1:RFP*, *NMY-2:GFP*; *mCherry:PH*, *NMY-2:GFP*; *mCherry:PH*; *ect-2 (ax751)*, *ect-2 (ax751)*; *AJM-1:GFP*; *mCherry:PH*; *nmy-2 (ne1490)*; *AJM-1:GFP*; *mCherry:PH*, and *ect-2 (ax751)*; *Pplx-2:GFP*. All strains were maintained at 15°C except for fluorescent strains, which were kept at 20°C.

2.2 Genetic crosses and RNAi

Genetic crosses were performed using standard protocols and Chi-square statistical analyses were used to assess genetic interactions. For crosses using *ts* strains, such as *ect-2* (*ax751*), *let-502* (*sb118*) and *nmy-2* (*ne1490*) crosses were performed at 20°C, and then F2 or F3 progeny were upshifted as L4 stage hermaphrodites to 25°C to assess lethality at restrictive temperature. To assess ventral enclosure phenotypes, *ts ect-2* or *nmy-2* mutant embryos were upshifted during dorsal intercalation, just prior to ventral enclosure, or during ventral enclosure as indicated. The *ts let-502* mutant is zygotic and late staged L4's and young adults were upshifted to obtain ventral enclosure phenotypes, since ventral enclosure occurs during the switch from maternal-zygotic *let-502* gene expression (Piekny et al., 2000). Maternal *ts* alleles of *let-502* are sterile or have very low brood sizes even at restrictive temperature and were not used in this study (Piekny et al., 2000). RNA-mediated interference was performed as previously described (Kamath et al., 2001), and clones specific for *ani-1* (Y49E10.19), *let-502* (C10H11.9; both provided by M. Glotzer, U. Chicago), *ani-2* (K10B2.5), *hmr-1* (W02B9), *unc-3* (Y16B4A) and *nmy-2* RNAi (F20G4; both provided by J. C. Labbé, IRIC Montreal) were used in this study.

2.3 Microscopy

Imaging was performed on embryos collected using established protocols (Wernike et al., 2012, Sulston et al., 1983). DIC imaging was performed using the LEICA DMI6000B microscope with the 40X/1.25 NA objective, capturing Z-stacks of 2 µm thickness every 10 minutes for 7 hours using a Hamamatsu Orca R2 camera, piezo Z/ASI stage (MadCityLab), and Volocity acquisition software (PerkinElmer). Embryos expressing AJM-1:GFP were imaged with the same microscope, but Z-stacks of 1 µm thickness from the ventral surface were acquired

with fluorescence using the GFP filter (Semrock) every 12 minutes. To prevent phototoxicity, the aperture was closed to 17%, and exposure times were kept <300 ms with gain (up to 100). Strains expressing GFP, RFP or mCherry also were imaged using the 60X/1.4 NA or 100X/1.45 NA objectives on an inverted Nikon Eclipse Ti microscope outfitted with the Livescan Sweptfield scanner (Nikon), piezo Z stage (Prior) and the Andor Ixon 897 camera, with Elements 4.0 acquisition software (Nikon), GFP filter or dual GFP/mCherry filter (Chroma) and the 488 and 561 lasers (100 mW; set between 10-25% power). Z-stacks of 0.5 μm thickness were collected from the ventral surface every 10 minutes. All imaging was performed at room temperature, or at 25°C using chambers (IBIDI or TOKAI HIT model INU-TIZ-F1) on the Leica DMI6000B or Sweptfield microscope, respectively.

2.4 Image Analysis

To examine the localization of NMY-2:GFP in embryos co-expressing mCherry:PH, the original image files were deconvolved using AutoQuant X3 (MediaCybernetics). Files were opened with metadata and deconvolved using adaptive (theoretical) PSF (blind deconvolution). The total number of iterations varied from 5-10 and the noise level was set to medium or high depending on the intensity of the fluorescent signal and the background. Deconvolved images were imported into IMARIS 7.7.2 (Bitplane) and 3D surface rendering was applied equally on Z-stack projections from NMY-2:GFP; mCherry:PH embryos. NMY-2:GFP was surface rendered without smoothening, the surface grain was set at 2 μm and the diameter of the largest sphere was set at 5 μm to minimize the number of objects. The objects were selected based on thresholds of intensity above background levels of intensity. When surface rendering mCherry:PH to reveal the cell boundaries, the surface rendering was smoothened, and the same

parameters were used as described above. Images also were collected after zooming in at 45-60° angles.

All measurements were performed in Image J (NIH Image) or Fiji. SeedWater Segmenter software (Mashburn et al., 2012) was used to track cells during closure of the ventral pocket. Deconvolved images of embryos expressing mCherry:PH were stacked to a thickness of 1 μm , to select the ventral-most layer of neuroblasts, and cells were tracked for 8-10 minutes. This software uses a watershed algorithm that tracks cells over time. Each cell is given an individual seed-point; this seed-point is assigned a colour and is tracked over time. Seed-points that move out of the plane of focus will retain their assigned colour in the form of a small square so as to denote the previous presence of that particular cell, even though it is no longer visible. Seed-points that share a common boundary will be assigned different colours, thus making it easier to observe their individual movements.

Chapter 3: Results

3.1 Non-muscle myosin accumulates as foci in the epidermal cells and neuroblasts during ventral enclosure

We wanted to determine how ventral enclosure is mechanically controlled. Prior studies showed that the ventral epidermal cells may require actin-myosin contractility, but myosin itself had not been studied during this stage of development. To characterize myosin during ventral enclosure, we first looked at its localization pattern. To accomplish this, we imaged embryos co-expressing GFP-tagged NMY-2 (non-muscle myosin heavy chain), with GFP integrated at the *nmy-2* gene locus by CRISPR-mediated genome editing, and mCherry:PH (localizes to plasma membranes) to outline the cell boundaries. We imaged embryos as they entered ventral enclosure and noticed that myosin foci accumulated at the junction-free edges of the ventral epidermal cells. The foci appeared to coalesce to form a uniform ring-like structure around the pocket that forms after the anterior leading edge cells meet at the midline (Figure 10). We also observed the accumulation of myosin foci in neuroblasts (neuronal precursor cells) within the pocket (Figure 10). We used Imaris software to surface render the images to more clearly see the patterning and position of myosin in the cells (myosin is in green and the cell boundaries are in red; Figure 10). These images showed how a myosin ring appears to form and close from the anterior to the posterior of the embryo.

By rotating the embryo and looking at it from a more lateral perspective, myosin appeared to localize near the ventral surface of both the epidermal cells and neuroblasts in the ventral pocket (Figure 11). We also zoomed in on the surface rendered embryos at a 45-60

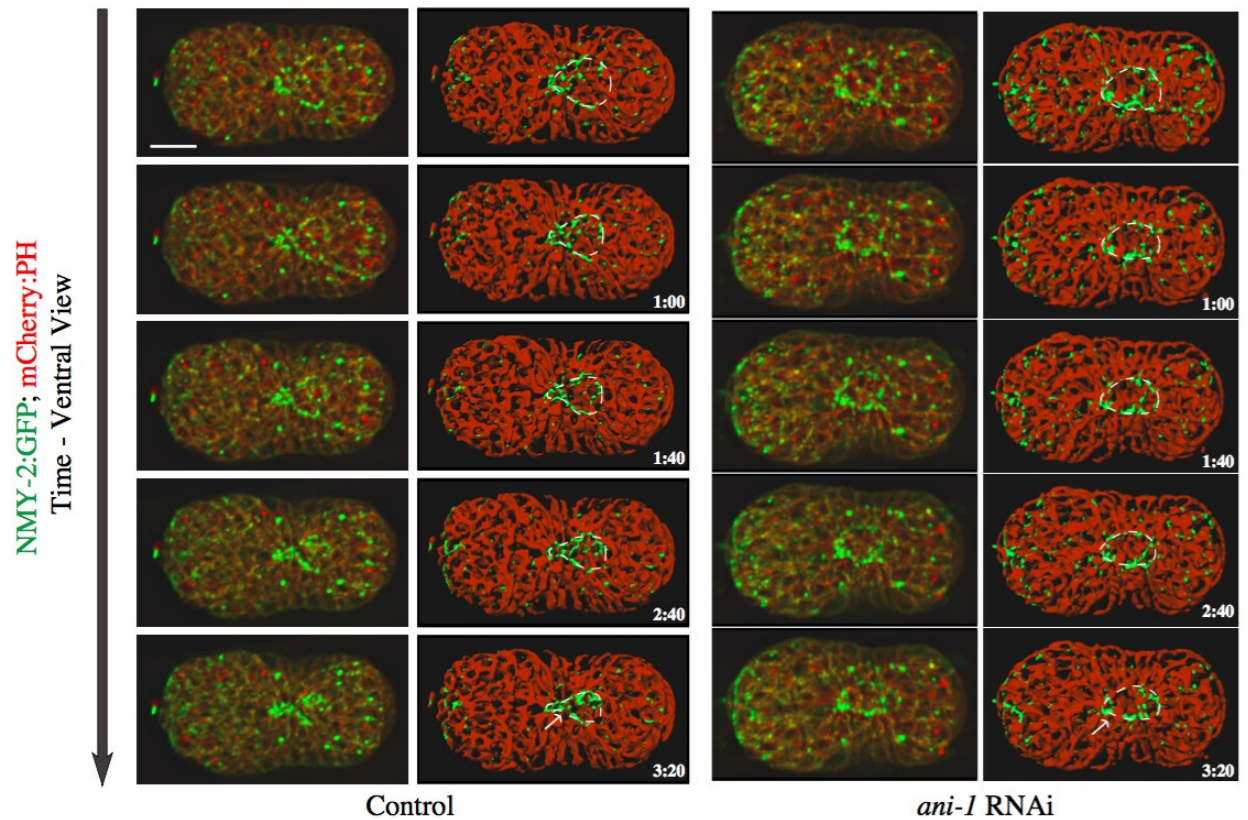


Figure 10. Non-muscle myosin localizes as networks of foci in epidermal cells and neuroblasts during ventral enclosure. Ventral views of 6 μm Z-stack projections (12 stacks of 0.5 μm thickness) of NMY-2:GFP; mCherry:PH control and *ani-1* RNAi embryos are shown after deconvolution over time (panels on the left; $11 < n < 13$). Projections of the deconvolved images were surface rendered for both channels (panels on the right) to clarify the cell boundaries and myosin patterns of localization. The white dotted line depicts the ventral pocket. The scale bar is 10 μm .

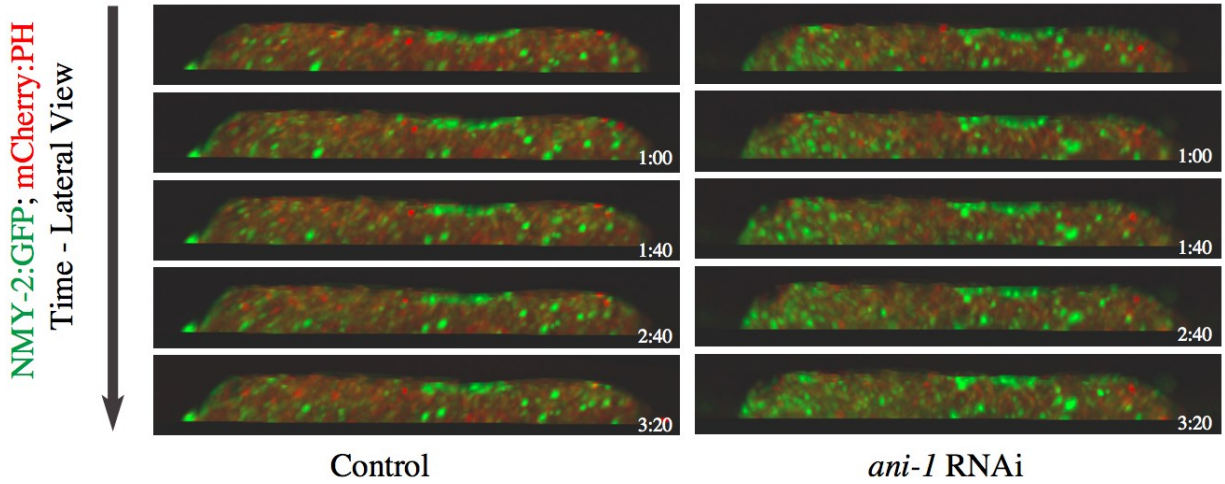


Figure 11. Myosin foci localize as foci near the ventral surface of the embryo. Lateral views of 6 μ m Z-stack projections of NMY-2:GFP; mCherry:PH control and *ani-1* RNAi embryos are shown after deconvolution over time ($11 < n < 13$).

degree angle from the top of the ventral pocket to get a better sense of myosin distribution in the cells in this region (Figure 12). Myosin appeared to be strongly accumulated near the ventral surface in a coordinated manner across several cells (Figure 12).

3.2 Non-muscle myosin activity is required for ventral enclosure

Next, we determined if myosin is required for ventral enclosure. We upshifted *nmy-2* (ts) mutant embryos prior to ventral enclosure and observed ventral enclosure defects (data not shown; in thesis by D. Wernike). In these embryos, the leading edge cells migrated toward the ventral midline, but the ventral pocket failed to close or was delayed. This phenotype also was observed in embryos with mutations (or after RNAi) in genes known to regulate myosin activity, including *ect-2* (Rho GEF) and *let-502* (Rho kinase; data not shown; in thesis by D. Wernike). We further examined changes in myosin localization in *ect-2* and *let-502* mutant or RNAi embryos. Indeed, in embryos with loss of *ect-2* or *let-502* function, there was a lower proportion of myosin fluorescence and foci in both the epidermal cells and neuroblasts (data not shown; in thesis by D. Wernike).

Since myosin foci accumulate in a subset of neuroblasts within the ventral pocket during ventral enclosure, we were interested in determining the role for myosin in the neuroblasts. To accomplish this, we used a *C. elegans* strain, *lin-15B* (*n744*); *uls57*, that selectively increases the sensitivity of the neuroblasts to RNAi treatment and decreases sensitivity of all other cell types to RNAi treatment. This strain contains an integrated transgene with *sid-1* (encodes a dsRNA-selective channel) and YFP controlled by the *unc-119* neuroblast promoter. Overexpression of the transmembrane protein SID-1 in the neuroblasts leads to an increase in dsRNA within these cells at the expense of other tissues (Calixto et al., 2010). We observed a range of phenotypes,

after exposing the *lin-15B* (*n744*); *uls57* worms to *nmy-2* RNAi, including ventral enclosure defects (data not shown; in thesis by D. Wernike). This demonstrates that myosin is required in the neuroblasts for ventral enclosure, but its function is not clear.

3.3 Neuroblasts in the ventral pocket reorganize during ventral enclosure

After discovering that myosin contractility is required in the neuroblasts, we wanted to further characterize the neuroblasts throughout ventral enclosure. To do this, we imaged AJM-1-GFP; mCherry:PH embryos, and we discovered that some neuroblasts in the ventral pocket form transient yet distinct patterns during pocket closure. The first step of this organization is when 6-8 neuroblasts form two columns, which is followed by their rearrangement into a circular pattern (rosette) with myosin foci enriched in a vertex shared by 5 cells (Figure 13). The assembly and disassembly of rosettes have been shown to mediate the elongation of epithelial tissues (Harding et al., 2014). Next, we used SeedWater Segmenter software to track individual cells over time. This software colour-codes cells, enabling us to follow each cell over time and see changes in their shape and association with neighbours. The software verified that a subset of neuroblasts in the ventral pocket undergo rearrangements during closure to form a circular, rosette-like pattern (Figure 13). Interestingly, networks of myosin align with cells in the rosette, and their surface area decreases during pocket closure (data not shown; in thesis of D. Wernike).

In other organisms, rosette formation is myosin-dependent and we determined if the changes in neuroblast organization during pocket closure also are myosin-dependent. To do this we imaged *nmy-2* (*ts*) mutant embryos co-expressing AJM-1-GFP and mCherry:PH upshifted to restrictive temperature either just before or during ventral enclosure. Embryos upshifted after the leading cells began to migrate caused delays in pocket closure (Figure 14). In the delayed

AJM-1::GFP; mCherry:PH

Zoom

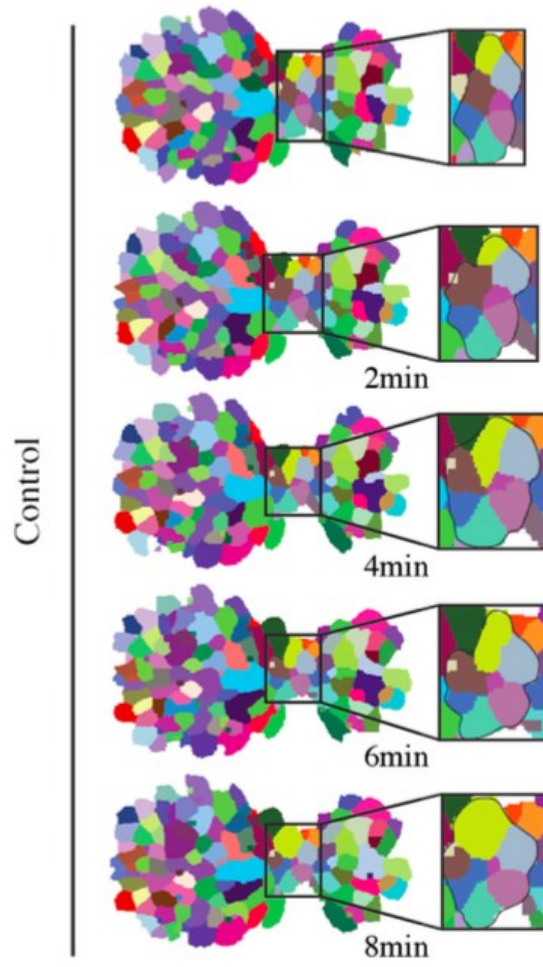
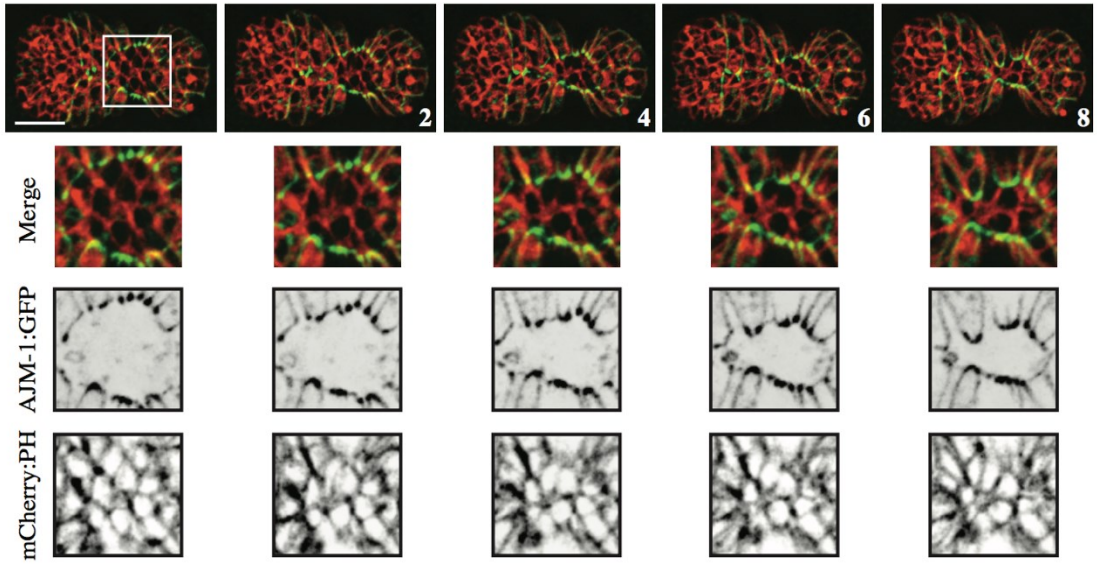
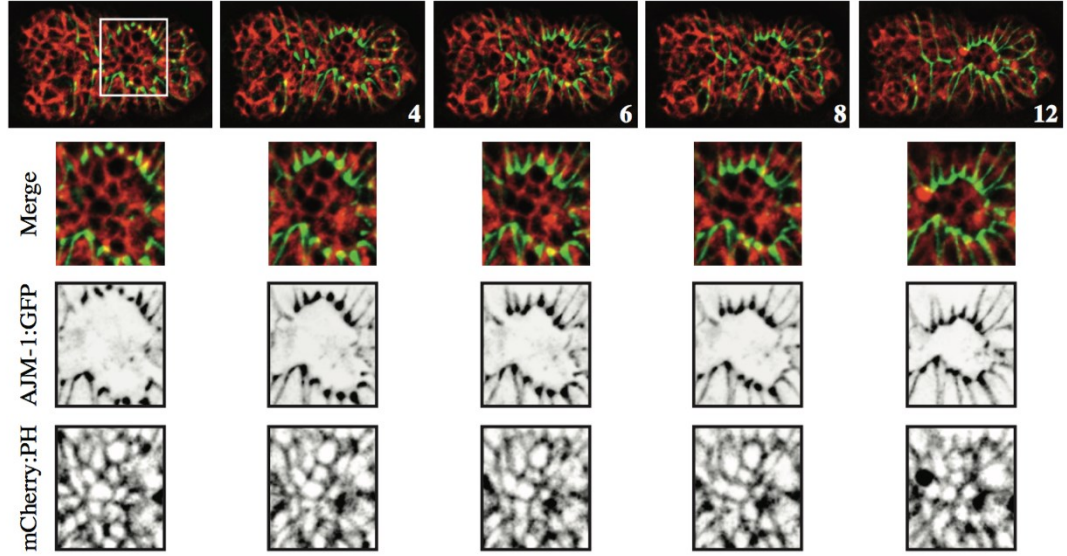


Figure 13. Neuroblasts in the pocket form rosettes during ventral enclosure. Images of AJM-1:GFP; mCherry:PH control embryos are shown during ventral enclosure over time (AJM-1 epidermal cell junctions in green and cell boundaries in red). The box shows the region that is zoomed in underneath with inverted images for each channel as well as the merged images as indicated. The scale bar is 10 μm and the time scale is in minutes. Each cell in the neuroblast focal plane (thickness of 1 μm from two Z planes) of an mCherry:PH-expressing control embryo. Embryo is colour-coded and tracked during pocket closure using Seedwater Segmenter software. The pocket region is outlined in a black box, and zoomed in to more clearly show the arrangement of cells in this region.

AJM-1:GFP; mCherry:PH;
nmy-2 (ne1490), 'late' upshift

Zoom



nmy-2 (ne1490), 'late' upshift

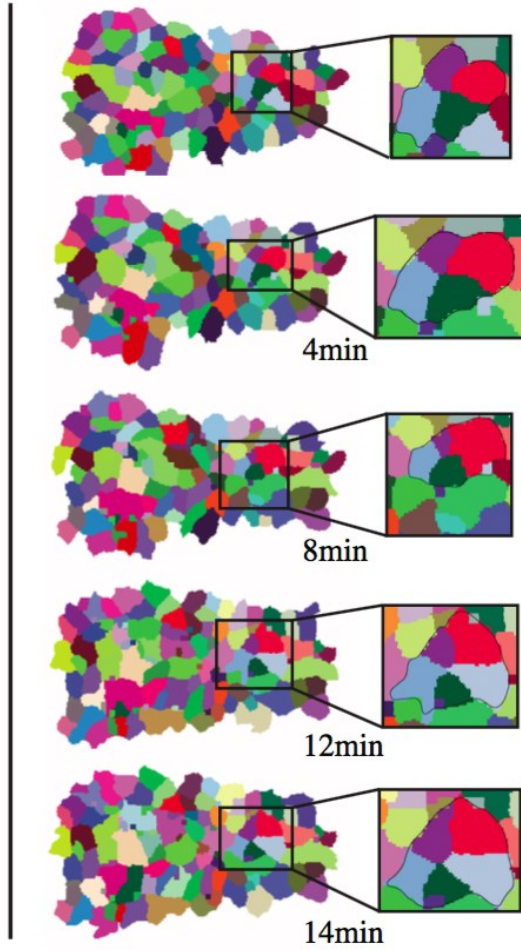


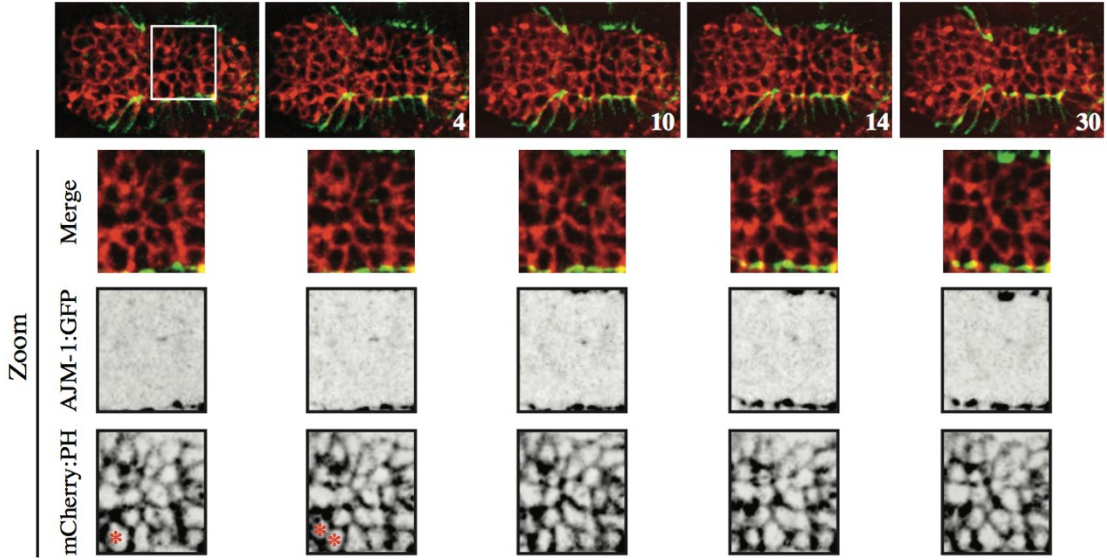
Figure 14. Neuroblasts form rosettes in ‘late’ myosin loss-of-function embryos. Image of AJM-1:GFP; mCherry:PH; *nmy-2 (ne1490)* embryo (‘late’ upshift). *nmy-2* mutant embryos were upshifted to restrictive temperature after the leading cells began migrating (‘late’ upshift). The box shows the region that is zoomed in underneath with inverted images for each channel as well as the merged images as indicated. The scale bar is 10 μm and the time scale is in minutes. Each cell in the neuroblast focal plane (thickness of 1 μm from two Z planes) of an mCherry:PH-expressing embryo is colour-coded and tracked during pocket closure using Seedwater Segmenter software. The pocket region is outlined in a black box, and zoomed in to more clearly show the arrangement of cells in this region.

embryos, the neuroblasts still form rosettes with 5 cells, but their surface area did not change as quickly as in control embryos (data not shown, in thesis of D. Wernike; Figure 14). Embryos that were upshifted just prior to ventral enclosure had failed pocket closure and the neuroblasts failed to form rosettes altogether (Figure 15). This data suggests that there may be different threshold and/or temporal requirements for myosin in the neuroblasts to mediate changes in their organization and surface area.

3.4 Neuroblast cell shape, number and organization are important factors for ventral enclosure

Since neuroblast organization is important for ventral pocket closure, we wanted to determine how selectively altering the division or fate of subsets of neuroblasts affects this process. We previously reported that *ani-1* (anillin) is required for ventral enclosure (Fotopoulos et al., 2013). It is expressed in and required for the division of a subset of neuroblasts, which may non-autonomously affect migration of the overlying ventral epidermal cells. We revisited these experiments to see the effect of *ani-1* RNAi on the distribution of myosin in epidermal cells and neuroblasts during ventral enclosure. In *ani-1* RNAi embryos, myosin was not distributed uniformly around the ventral pocket, and the ring was more asymmetric (Figure 10). Also, surface rendering revealed that the ring failed to close in an anterior-posterior fashion (Figure 10). Lateral views of Z-projections showed that myosin foci no longer appeared to accumulate only near the ventral surface of cells in the ventral pocket, and were also found more dorsally (Figure 11). By zooming in on surface rendered *ani-1* RNAi embryos at a 45-60 degree angle from the top of the ventral pocket, we found that myosin was no longer uniformly distributed across multiple cells as in control embryos (Figure 12).

AJM-1:GFP; mCherry:PH;
nmy-2 (ne1490), 'early' upshift



nmy-2 (ne1490), 'early' upshift

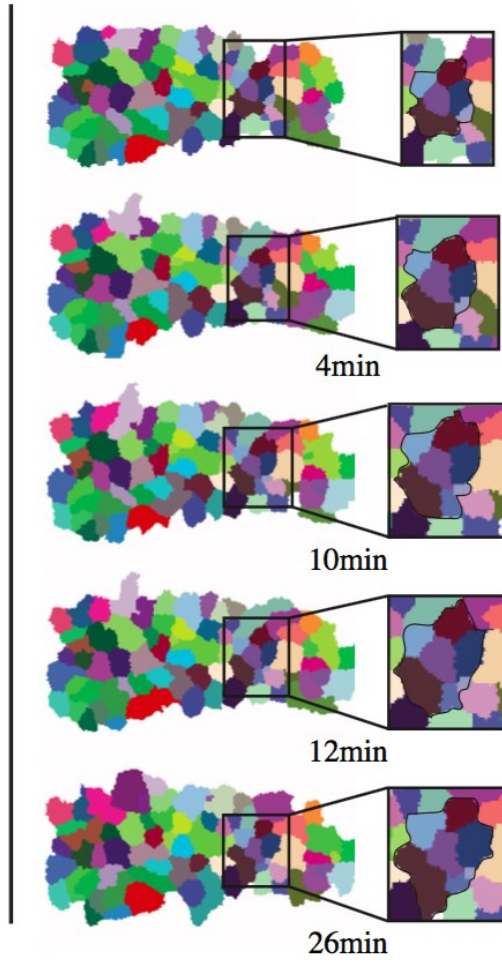


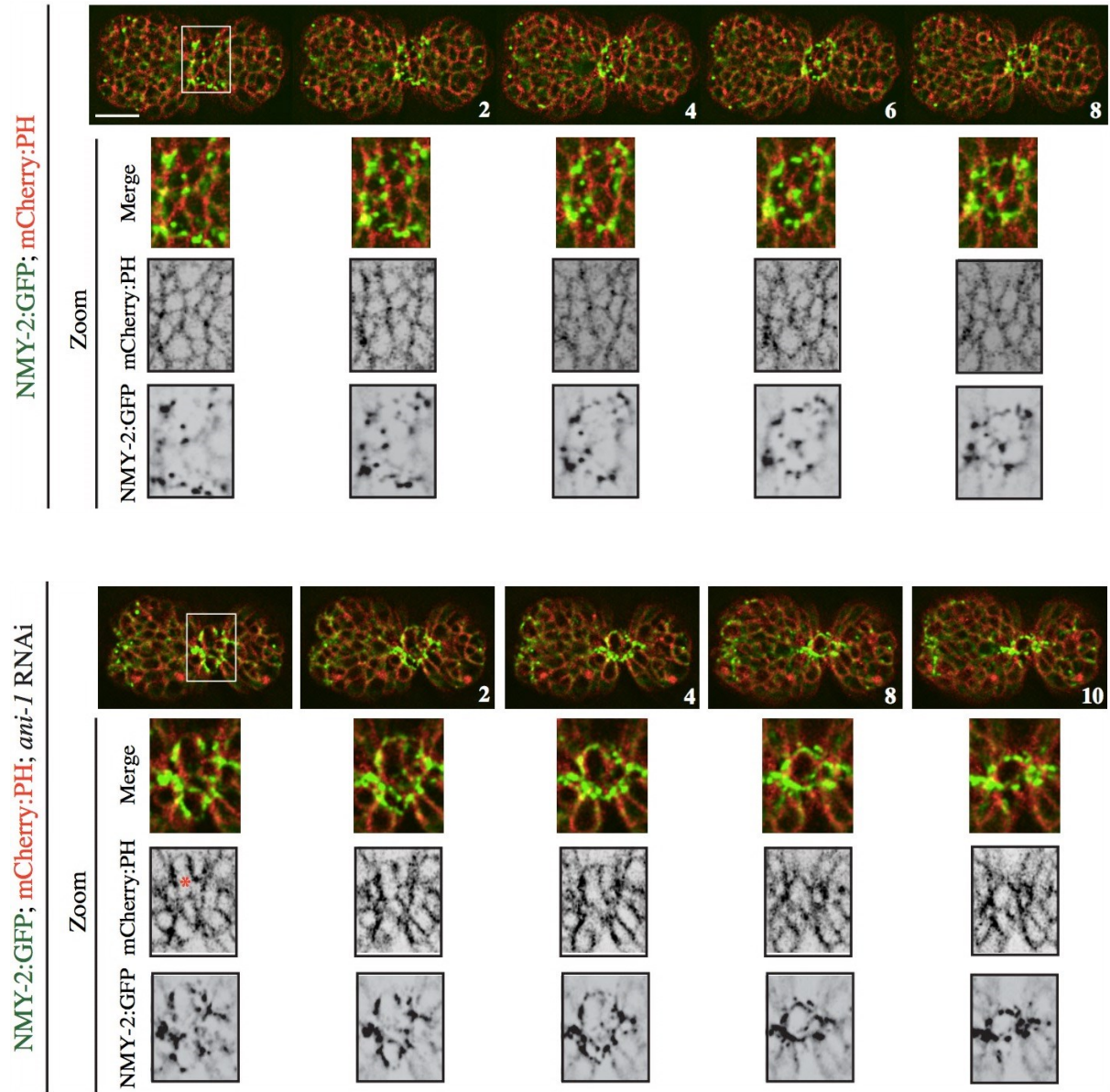
Figure 15. Neuroblasts do not form rosettes in ‘early’ myosin loss-of-function embryos.

Image of AJM-1:GFP; mCherry:PH; *nmy-2 (nel490)* embryo (‘early’ upshift). *nmy-2* mutant embryos were upshifted to restrictive temperature after the leading cells began migrating (‘early’ upshift). The box shows the region that is zoomed in underneath with inverted images for each channel as well as the merged images as indicated. The red asterisk depicts a neuroblast cell that undergoes successful division. The scale bar is 10 μm and the time scale is in minutes. Each cell in the neuroblast focal plane (thickness of 1 μm from two Z planes) of an mCherry:PH-expressing embryo is colour-coded and tracked during pocket closure using Seedwater Segmenter software. The pocket region is outlined in a black box, and zoomed in to more clearly show the arrangement of cells in this region.

We also examined the effect of *ani-1* RNAi on neuroblast organization during ventral enclosure, to determine how this could correlate with changes in the migration of the overlying epidermal cells. In *ani-1* RNAi embryos, the neuroblasts appeared misshapen, likely due to cytokinesis failure, and they formed an oddly organized rosette with only 4 cells vs. 5 cells in control embryos (Figure 16A). Also, the neuroblasts failed to decrease in surface area at the same rate as in control embryos (data not shown; in thesis of D. Wernike). We also observed that myosin distribution was uneven in both the epidermal cells and neuroblasts, which correlated with changes in their movements and organization (Figure 16B).

Since *ani-1* could be required in the epidermal cells, even though it is not highly expressed in these cells, we wanted to perturb the neuroblasts in another way to test their requirement for ventral enclosure. We imaged embryos with mutations in different genes known to alter neuroblast cell fate. Interestingly, some had no ventral enclosure phenotypes, such as *fax-1* (nuclear receptor expressed in and required for the fate of AVA, AVE and AVK neurons; Wightman et al., 2005) or *cnd-1* (NeuroD transcription factor required for motor neuron fate; Hallam et al., 2000). Others, such as *unc-3* (encodes a transcription factor specifically required for neurons from the RID lineage, Wang et al., 2015) and *hlh-14/mnCI* (encodes an Achaete-Scute bHLH homologue specifically expressed in the PVQ/HSN/PHB neuroblasts, Frank et al., 2003) caused a range of ventral enclosure phenotypes (Figure 17). These include rupture (2.6%, n=38 *unc-3*), delayed ventral enclosure (10.5% *unc-3*; 16.3, n=43 *hlh-14/mnCI*) and Vab (variable abnormal body morphology; 2.6% *unc-3*; 2.3% *hlh-14/mnCI*) phenotypes, respectively (Figure 17). Imaging myosin localization in NMY-2:GFP embryos treated with *unc-3* RNAi showed that similar to *ani-1*-depleted embryos, myosin was more unevenly distributed around the ventral pocket, which closed more asymmetrically (Figure 18). However, the *unc-3* RNAi

A



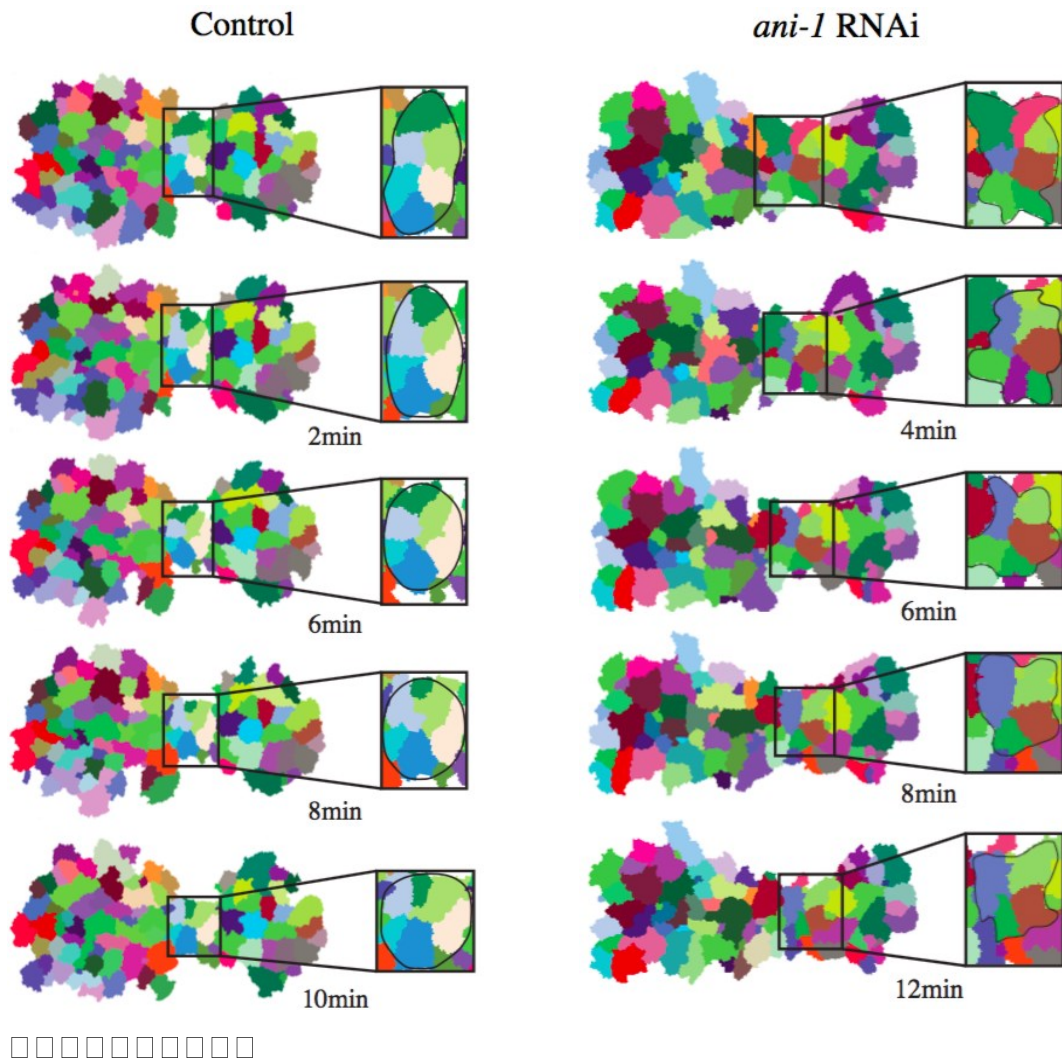
B

Figure 16. Disrupting neuroblast division alters myosin distribution during ventral enclosure. **A)** Images of NMY-2:GFP; mCherry:PH from control and *ani-1* RNAi embryos are shown during ventral enclosure ($9 < n < 11$). The rosette-like pattern formed between neuroblasts correlates with the accumulation of myosin at a central focal point (vertex). The box shows the region that is zoomed in underneath with inverted images for each channel as well as the merged images as indicated. The scale bar is $10 \mu\text{m}$ and the time scale is in minutes. **B)** Each cell in the neuroblast focal plane (thickness of $1 \mu\text{m}$ from two Z planes) of an mCherry:PH-expressing control or *ani-1* RNAi embryo is colour-coded and tracked during pocket closure using Seedwater Segmenter software. The pocket region is outlined in a black box, and zoomed in to more clearly show the arrangement of cells in this region.

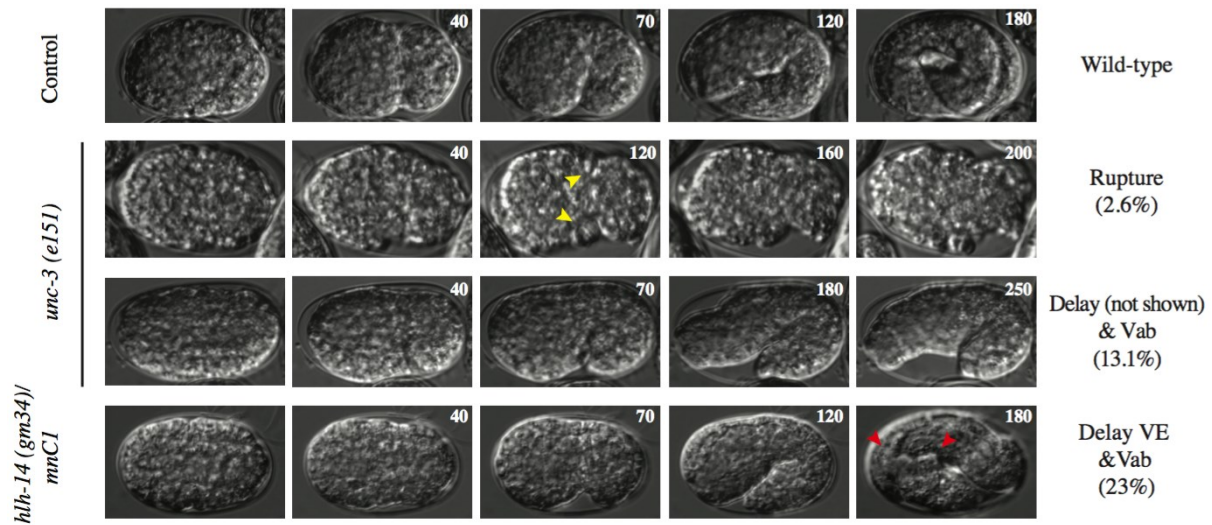


Figure 17. Neuroblast fate is important for ventral enclosure. DIC time lapses of *unc-3 (e151)* and *hll-14 (gm34)/mnC1* mutant embryos are shown during ventral enclosure ($38 < n < 43$). Yellow arrowheads point to ventral epidermal cells and the red arrowheads point to sites of abnormal body morphology (Vab). The phenotypes and their proportions are indicated on the right. The scale bar for all embryos is 10 μm and the time scale is in minutes.

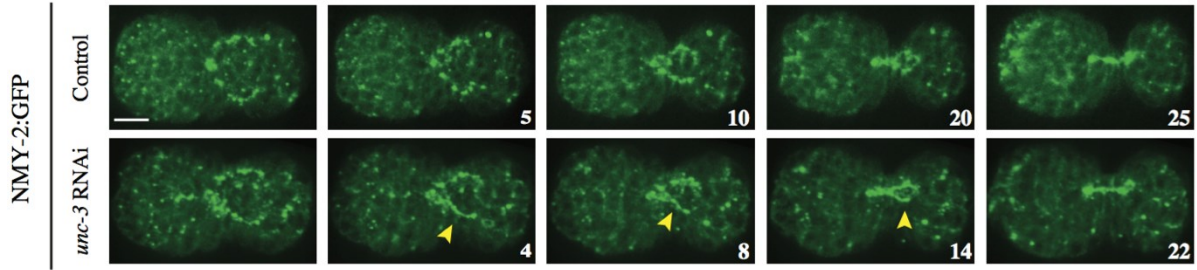


Figure 18. Altering neuroblast fate influences myosin localization during ventral enclosure.

Time lapse images of a NMY-2:GFP-expressing control and *unc-3(e151)* embryo are shown during ventral enclosure. The yellow arrowhead point to ventral epidermal cells that partially lag behind during pocket closure. The scale bar is 10 μ m and the time scale is in minutes.

ventral enclosure phenotypes were not as strong as the allele, likely because neuronal-specific RNAi is typically not very effective. Regardless, our data suggests that the reorganization of a subset of neuroblasts may be important for ventral enclosure by influencing the distribution of myosin and the movement of the overlying epidermal cells.

3.5 α -catenin localizes to neuroblast cell boundaries during ventral enclosure

We wanted to determine how myosin contractility could mediate changes in neuroblast reorganization for ventral enclosure. Since myosin is required for rosette formation, it likely is driving changes in cell shape or movement. However, to transmit forces into cell shape changes or movement, actomyosin filaments need to be anchored to adhesion junctions (Armenti et al., 2012). Adherens junctions have not been previously studied or described in *C. elegans* neuroblasts, although they have a neuronal-specific isoform of cadherin that is expressed after embryogenesis (Broadbent and Pettitt, 2012). To determine if adhesion junction proteins are present in the neuroblasts, we imaged α -catenin tagged with GFP (HMP-1:GFP) in embryos that co-express DLG-1-RFP during ventral enclosure. α -catenin localized to the boundaries of epidermal cells and neuroblasts during ventral enclosure. Interestingly, as the neuroblasts formed a rosette, α -catenin became enriched at the vertex, similar to myosin, which coincided with shrinking junctions between neighbouring cells (Figure 19). Further, in embryos treated with *hmr-1* (E-cadherin) RNAi, the surface area of the neuroblasts failed to change as quickly as in control embryos (data not shown), and rosettes formed, but in some embryos they varied in comparison to control embryos (Figure 20). Therefore, although preliminary, our data suggests that the neuroblasts are associated with one another via adherens junctions, which change as the neuroblasts form rosettes.

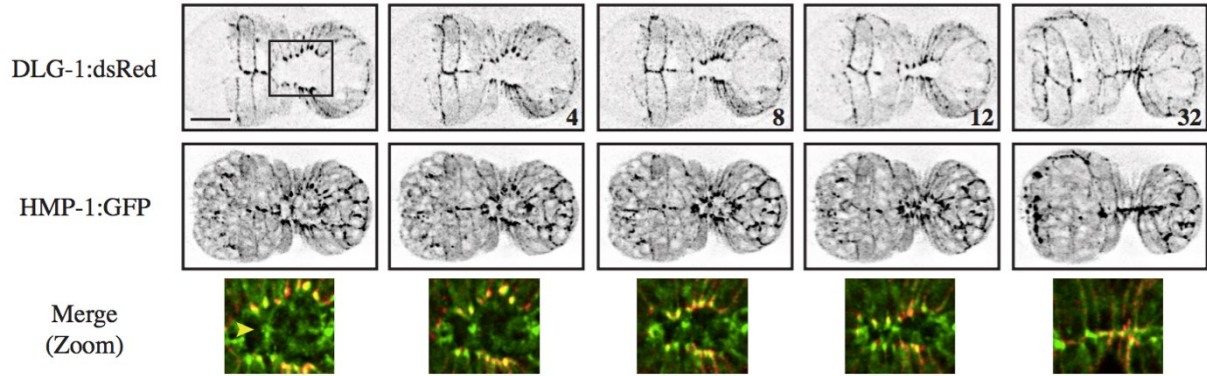


Figure 19. The adherens junction protein α -catenin accumulates in re-organizing neuroblasts during ventral enclosure. Images of an HMP-1:GFP; DLG-1:dsRed embryo is shown during ventral enclosure. Each channel is inverted, and the box shows the region zoomed in underneath as merged images. The scale bar is 10 μ m and the time scale is in minutes.

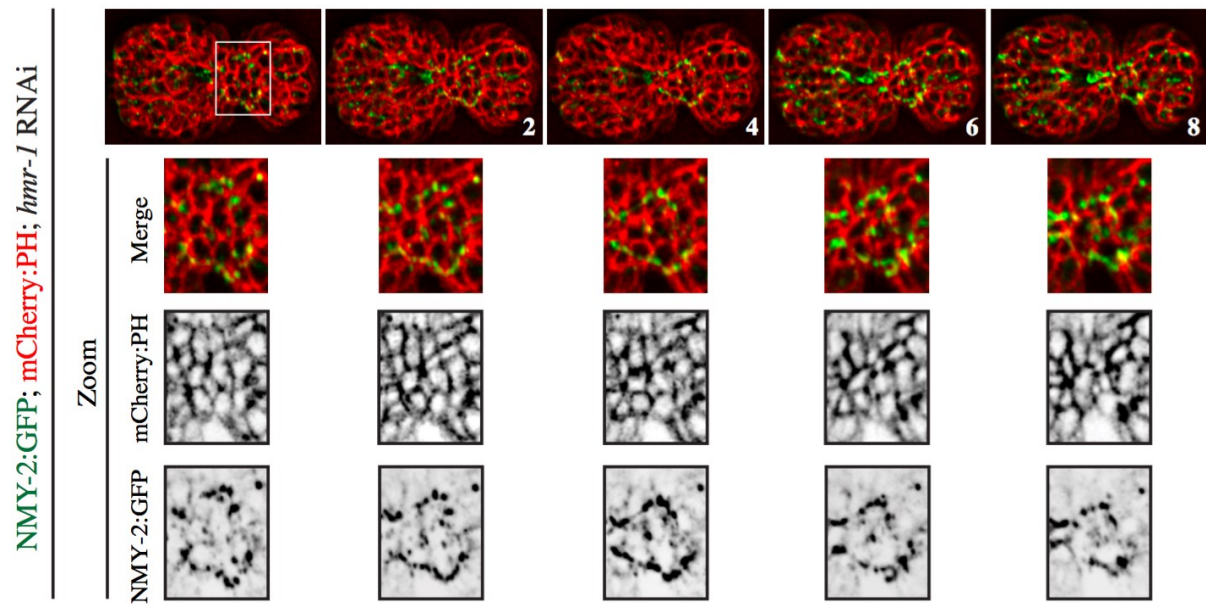


Figure 20. Neuroblasts form disorganized rosettes after mild disruption of *hmr-1*/E-cadherin function. Images of NMY-2:GFP; mCherry:PH; *hmr-1* RNAi. Embryos are shown during ventral enclosure over time. The box shows the region that is zoomed in underneath with inverted images for each channel as well as the merged images as indicated. The scale bar is 10 μ m and the time scale is in minutes.

Chapter 4: Discussion

We found that myosin may be required for neuroblast and epidermal morphogenesis during *C. elegans* development. During part of epidermal morphogenesis, ventral enclosure, the epidermal cells cover the ventral surface of the embryo using cues from the underlying neuroblasts (Chisholm and Hardin, 2005). As the posterior ventral epidermal cells move to cover the ventral surface, they constrict at their junction-free ends to form a pocket (Williams-Masson et al., 1997). F-actin cables form a supracellular ring around this pocket, and our data shows that contractile myosin foci also are enriched in this ring, suggesting that it constricts via contractility (Williams-Masson et al., 1997; Chisholm and Hardin, 2005; Zhang et al., 2010). In addition, we found that myosin contractility regulates changes in the organization and surface area of the neuroblasts in the pocket. Further, these cells influence the localization of myosin in the overlying epidermal cells. Although different cell types are involved, we can draw parallels with dorsal closure in *Drosophila*. During dorsal closure, the extraembryonic amnioserosa tissue is required for closure of the epidermis on the back of the embryo (Franke et al., 2005). During this process, extensive myosin contractility constricts the amnioserosal cells to decrease their surface area and influences contractility of the actin-myosin ring in the overlying dorsal epidermal cells (Franke et al., 2005). Therefore, the neuroblasts may be instrumental for pocket closure by either shrinking in surface area, which brings the overlying cells closer together, and/or they may generate tension that influences the epidermal cells via mechanosensing (Figures 21; 22).

During closure of the ventral pocket, we observed myosin accumulate as foci into a ring-like pattern around the junction-free edges of the ventral pocket epidermal cells. The foci form an interconnected network near the ventral surface of the cells similar to a pattern that has been observed for actin (Williams-Masson, 1997; Pollard et al., 2000; Amann and Pollard, 2007;

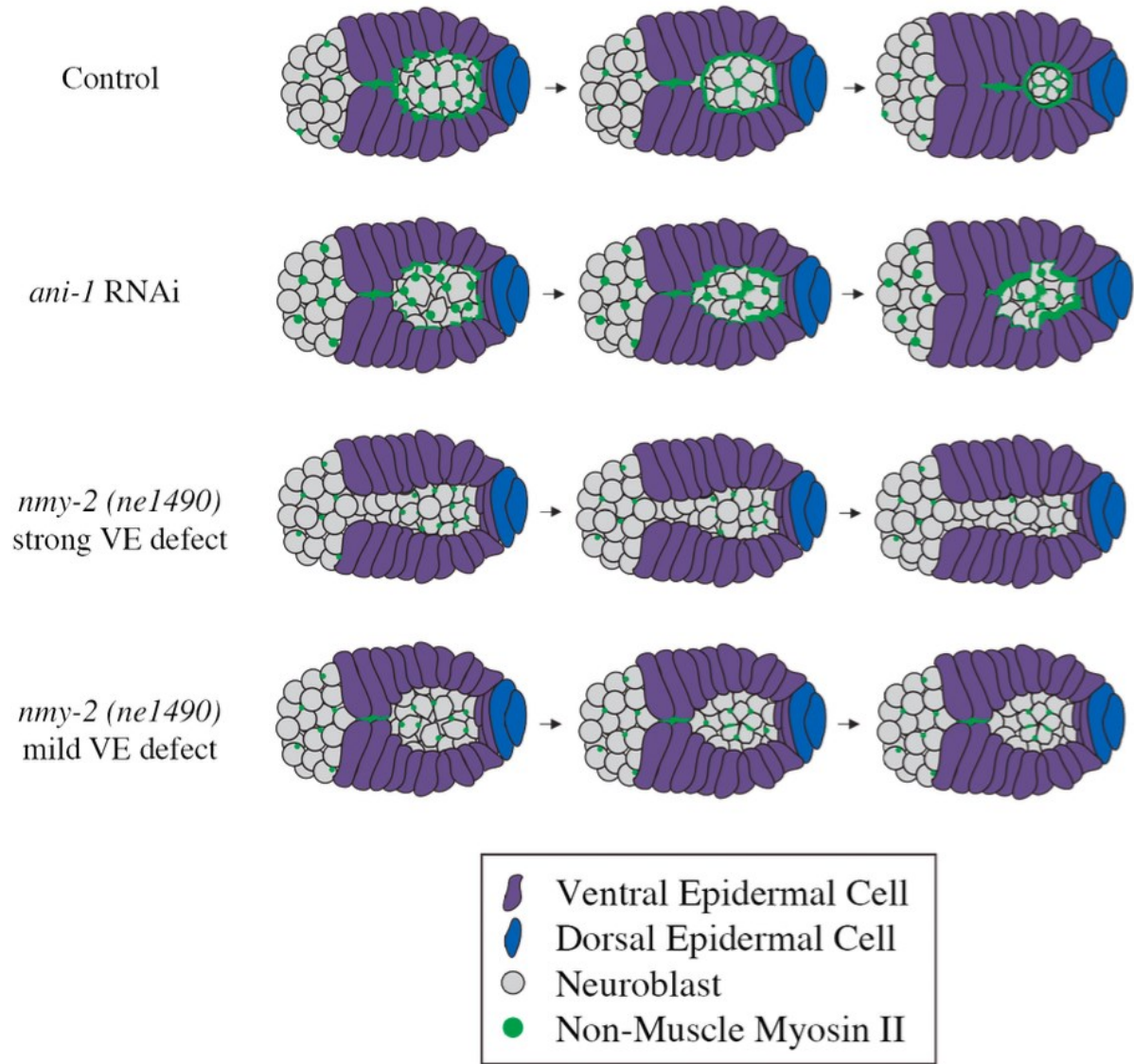


Figure 21. Model for myosin regulation and neuroblast organization during ventral enclosure. Cartoon models show the changes in myosin localization and neuroblast organization as the ventral pocket closes in control, *ani-1* RNAi and *nmy-2 (ne1490)*, strong and mild) mutant embryos.

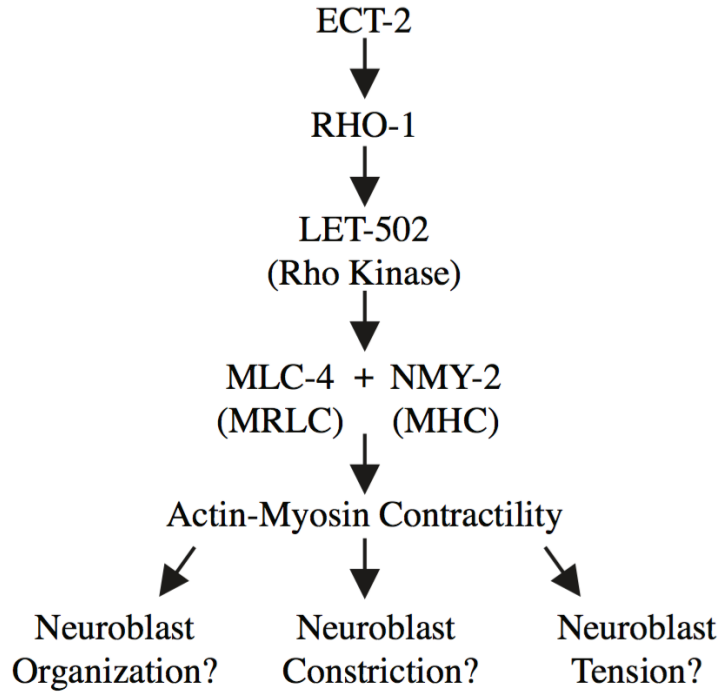


Figure 22. Pathway for myosin regulation and neuroblast organization during ventral enclosure. The molecular pathway regulating actin-myosin contractility in the neuroblasts is shown. This pathway could influence neuroblast organization, neuroblast constriction, or generate tension, all of which could contribute to ventral enclosure.

Goley and Welch, 2006). This localization pattern supports a previously described model that this ring closes via actin-myosin contractility. Indeed, we observed that this ring either fails to constrict or is delayed in embryos with mutations in genes regulating myosin contractility, or in myosin itself.

Interestingly, we also observed myosin accumulate as networks of foci in the underlying neuroblasts. Previous studies showed that the neuroblasts sort from one another to form distinct pools of cells either expressing the ephrin ligand, or the ephrin receptor (Chin-Sang et al., 1999; Chin-Sang et al., 2002). Further, they provide chemical cues to mediate migration of the overlying epidermal cells (Roy et al., 2000; Ikegami et al., 2012). However, the role of mechanical forces has not been investigated in the neuroblasts, which are commonly depicted as ‘circular balls’ underneath the epidermis. We found that myosin is specifically required in the neuroblasts for successful ventral enclosure, suggesting that mechanical forces are important in these cells for this process. However, the role of myosin is still not clear. Our data shows that the neuroblasts reorganize during ventral enclosure, where they start out as columns, then form rosettes, and possibly resolve into rows (although we were not able to see this). Also, a previous student in the lab found that the surface area of the neuroblasts shrinks during pocket closure. Still, it is not clear how their surface area shrinks; either the cells apically constrict or they may ingress into the embryo. Myosin is required for both of these processes and failure of the neuroblasts to undergo these changes disrupts closure of the overlying epidermis. For myosin to transmit forces into cell shape changes or movements, the actomyosin filaments need to be anchored at junctions. We observed the localization of an adherens junction marker in the neuroblasts and found that it is strikingly similar to the localization pattern of myosin. As the neuroblasts organize into the rosette pattern, their shape becomes more wedge-shaped and the

junction markers change accordingly, since their associations with neighbouring cells also changes. This is the first description, to our knowledge, of the neuroblasts undergoing morphogenetic events, and that these cells are tethered via junctions.

We further assessed the role of the neuroblasts in influencing closure of the overlying epidermal cells. Using *ani-1* RNAi to cause neuroblast cell division defects and alter neuroblast cell shape (Fotopoulos et al., 2013), we found that myosin was asymmetrically distributed along the edges of the epidermal cells, which displayed defective closure and epidermal cell misalignment. Further, when we perturbed the fate of a subset of neuroblasts using *unc-3* and *hlh-14*, we observed clear ventral enclosure phenotypes, similar to *ani-1* RNAi. Previous studies revealed that myosin accumulates in response to mechanical stress (Neujahr et al., 1997; Fernandez-Gonzalez et al., 2009). For example, during *Drosophila* germband extension, introducing ectopic forces using microaspiration induced the recruitment of myosin to the apical surface of cells (Fernandez-Gonzalez et al., 2009). Other studies have shown that actin-myosin activity in cells can change in response to changes in the rigidity of their environment, possibly via stretch-sensitive adhesion proteins (Fouchard et al., 2011). Therefore, this supports our model that the neuroblasts provide a critical role for effective ventral enclosure, possibly by generating tension that is mechanosensed by the overlying epidermal cells (Figures 21; 22).

Our data raises the importance of studying tissue morphogenesis in vivo, by considering multiple tissues undergoing morphogenesis concomitantly vs. single tissues in vitro. Few studies have been able to do this, and further, it has been difficult to study the role of mechanical forces in morphogenesis. As described earlier, *Drosophila* dorsal closure occurs due to the zippering of actin-myosin at the leading edges of the dorsal-most epidermal cells, which is influenced by apical constrictions in the underlying amnioserosa. Interestingly, *C. elegans* ventral enclosure

involves a second tissue, the neuroblasts, which are non-epidermal. However, they form adhesion junctions, which may coordinate changes in their movement or shape. Also, they undergo changes in their organization, and it is not clear if this helps coordinate actin-myosin filaments to generate tension that is sensed by the overlying epidermis and/or strictly helps to elongate the tissue. We are well-positioned to now study the model that the neuroblasts provide tension for mechanosensing.

Chapter 5: References

Amann, K.J. and Pollard, T.D., 2001. **Cellular regulation of actin network assembly.** *Curr Biol* 10: R728-R730

Amann, K.J. and Pollard, T.D., 2001. **Direct real-time observation of actin filament branching mediated by Arp2/3 complex using total internal reflection microscopy.** *PNAS USA* 98: 15009–15013.

Amano, M., Ito, M., Kimura, K., Fukata, Y., Chihara, K., Nakano, T., Matsuura, Y., Kaibuchi, K., 1996. **Phosphorylation and activation of myosin by Rho-associated kinase (Rho-kinase).** *J Biol Chem* 271: 20246-20249.

Amini, R., Goupil, E., Labella, S., Zetka, M., Maddox, A.S., Labbe, J.C., Chartier, N.T., 2014. **C. elegans Anillin proteins regulate intercellular bridge stability and germline syncytial organization.** *J Cell Biol* 206: 129-143

Armenti, S.T. and Nance, J., 2012. **Adherens junctions in C. elegans morphogenesis.** *Subcell Biochem* 60: 279-299.

Bernadskaya, Y.Y., Wallace, A., Nguyen, J., Mohler, W.A. and Soto, M.C., 2012. **UNC-40/DCC, SAX-3/Robo, and VAB-1/Eph polarize F-actin during embryonic morphogenesis by regulating the WAVE/SCAR actin nucleation complex.** *PLoS Genet* 8: e1002863.

Blankenship, J.T., Backovic, S.T., Sanny, J.S., Weitz, O., Zallen, J.A., 2006. **Multicellular rosette formation links planar polarity to tissue morphogenesis.** *Dev Cell* 11: 459-470.

Brenner. S., 1974. **The genetics of *Caenorhabditis elegans*.** *Genetics* 77: 71-94.

Broadbent, I.D., Pettitt, J., 2002. **The *C. elegans hmr-1* gene can encode a neuronal classic cadherin involved in the regulation of axon fasciculation.** *Curr Biol* 12: 59-63.

Costa, M., Raich, W., Agbunag, C., Leung, B., Hardin, J. and Priess, J.R., 1998. **A putative catenin-cadherin system mediates morphogenesis of the *Caenorhabditis elegans* embryo.** *J Cell Biol* 141: 297-308.

Chin-Sang, I.D., George, S.E., Ding, M., Moseley, S.L., Lynch, A.S. and Chisholm, A.D., 1999. **The ephrin VAB-2/EFN-1 functions in neuronal signaling to regulate epidermal morphogenesis in *C. elegans*.** *Cell* 99: 781-790.

Chin-Sang, I.D. and Chisholm, A.D., 2000. **Form of the worm: genetics of epidermal morphogenesis in *C. elegans*.** *Trends Genetics* 16: 544-551.

Chin-Sang, I.D., Moseley, S.L., Ding, M., Harrington, R.J., George, S.E. and Chisholm, A.D., 2002. **The divergent *C. elegans* ephrin EFN-4 functions in embryonic morphogenesis in a pathway independent of the VAB-1 Eph receptor.** *Development* 129: 5499-5510.

Chisholm, A.D. and Hardin, J., 2005. **Epidermal morphogenesis.** *WormBook: the online review of *C. elegans* biology:* 1-22.

Fernandez-Gonzalez, R., Simoes Sde, M., Röper, J.C., Eaton, S., Zallen, J.A., 2009. **Myosin II dynamics are regulated by tension in intercalating cells.** *Dev Cell* 17: 736-743.

Fotopoulos, N., Wernike, D., Chen, Y., Makil, N., Marte, A. and Piekny, A., 2013. ***Caenorhabditis elegans* anillin (*ani-1*) regulates neuroblast cytokinesis and epidermal morphogenesis during embryonic development.** *Dev Biol* 383: 61-74.

Fouchard, J., Mitrossilis, D. and Asnacios, A., 2011. **Actomyosin based response to stiffness and rigidity sensing**. *Cell Adh Migr* 5: 16-19.

Franke, J.D., Montague, R.A. and Kiehart, D.P., 2005. **Nonmuscle myosin II generates forces that transmit tension and drive contraction in multiple tissues during dorsal closure**. *Curr Biol* 15: 2208-2221.

Gally, C., Wissler, F., Zahreddine, H., Quintin, S., Landmann, F. and Labouesse, M., 2009. **Myosin II regulation during *C. elegans* embryonic elongation: LET-502/ROCK, MRCK-1 and PAK-1, three kinases with different roles**. *Development* 136: 3109-3119.

Goley, E.D. and Welch, M.D., 2006. **The ARP2/3 complex: an actin nucleator comes of age**. *Nat Rev Mol Cell Biol* 7: 713-726.

Hallam, S., Singer, E., Waring, D., Jin, Y., 2000. **The *C. elegans* NeuroD homolog *cnd-1* functions in multiple aspects of motor neuron fate specification**. *Development* 127: 4239-4252.

Harding, M.J., McGraw, H.F. and Nechiporuk, A., 2014. **The roles and regulation of multicellular rosette structures during morphogenesis**. *Development* 141: 2549-2558.

Harris, T.J. and Tepass, U., 2010. **Adherens junctions: from molecules to morphogenesis**. *Nature Rev Mol Cell Biol* 11: 502-514.

Ikegami, R., Simokat, K., Zheng, H., Brown, L., Garriga, G., Hardin, J., et al., 2012. **Smaphorin and Eph receptor signaling guide a series of cell movements for ventral enclosure in *C. elegans***. *Curr Biol* 22: 1-11.

Ishizaki, T., Maekawa, M., Fujisawa, K., Okawa, K., Iwamatsu, A., Fujita, A., Watanabe, N., Saito, Y., Kakizuka, A., Morii, N., Narumiya, S., 1996. **The small GTP-binding protein Rho binds to and activates a 160 kDa Ser/Thr protein kinase homologous to myotonic dystrophy kinase.** *EMBO J* 15: 1885-1893.

Kamath, R.S., Martinez-Campos, M., Zipperlen, P., Fraser, A.G., Ahringer, J., 2001. **Effectiveness of specific RNA-mediated interference through ingested double-stranded RNA in *Caenorhabditis elegans*.** *Genome Biol* 2: RESEARCH0002.

Kiehart, D.P., Galbraith, C.G., Edwards, K.A., Rickoll, W.L. and Montague, R.A., 2000. **Multiple forces contribute to cell sheet morphogenesis for dorsal closure in *Drosophila*.** *J Cell Biol* 149: 471-490.

Labouesse, M., 2006. **Epithelial junctions and attachments.** WormBook: the online review of *C. elegans* biology: 1-21.

Lecuit, T., Lenne, P.F., 2007. **Cell surface mechanics and the control of cell shape, tissue patterns and morphogenesis.** *Nat Rev Mol Cell Biol* 8: 633-644.

Maddox, A.S., Habermann, B., Desai, A. and Oegema, K., 2005. **Distinct roles for two *C. elegans* anillins in the gonad and early embryo.** *Development* 132: 2837-2848.

Maddox, A.S., Lewellyn, L., Desai, A. and Oegema, K., 2007. **Anillin and the septins promote asymmetric ingression of the cytokinetic furrow.** *Dev Cell* 12: 827-835.

Mashburn DN, Lynch HE, Ma X, Hutson MS., 2012 **Enabling user-guided segmentation and tracking of surface-labeled cells in time-lapse image sets of living tissues.** *Cytometry* 81: 409-418.

Matsumura, F., 2005. **Regulation of myosin II during cytokinesis in higher eukaryotes.** Trends Cell Biol 15: 371-377.

Neujahr, R., Heizer, C., Albrecht, R., Ecke, M., Schwartz, J.M., Weber, I., Gerisch, G., 1997. **Three-dimensional patterns and redistribution of myosin II and actin in mitotic *Dictyostelium* cells.** J Cell Biol 139: 1793-1804.

Patel, F.B., Bernadskaya, Y.Y., Chen, E., Jobanputra, A., Pooladi, Z., Freeman, K.L., et al., 2008. **The WAVE/SCAR complex promotes polarized cell movements and actin enrichment in epithelia during *C. elegans* embryogenesis.** Dev Biol 324: 297-309.

Piekny, A.J., Wissmann, A. and Mains, P.E., 2000. **Embryonic morphogenesis in *Caenorhabditis elegans* integrates the activity of LET-502 Rho-binding kinase, MEL-11 myosin phosphatase, DAF-2 insulin receptor and FEM-2 PP2c phosphatase.** Genetics 156: 1671-1689.

Piekny, A.J., Johnson, J.L., Cham, G.D. and Mains, P.E., 2003. **The *Caenorhabditis elegans* nonmuscle myosin genes *nmy-1* and *nmy-2* function as redundant components of the *let-502*/Rho-binding kinase and *mel-11*/myosin phosphatase pathway during embryonic morphogenesis.** Development 130: 5695-5704.

Piekny, A.J. and Maddox, A.S., 2010. **The myriad roles of Anillin during cytokinesis.** Sem Cell Dev Biol 21: 881-891.

Pollard, T.D., 2007. **Regulation of actin filaments assembly by Arp2/3 complex and formins.** Annu Rev Biophys Biomol Struct 36: 451-457.

Priess, J.R. and Hirsh, D.I., 1986. ***Caenorhabditis elegans* morphogenesis: the role of the cytoskeleton in elongation of the embryo.** Dev Biol 117: 156-173.

Roh-Johnson, M., Shemer, G., Higgins, C.D., McClellan, J.H., Werts, A.D., Tulu, U.S., et al., 2012. **Triggering a cell shape change by exploiting preexisting actomyosin contractions.** Science 335: 1232-1235.

Roy, P.J., Zheng, H., Warren, C.E., Culotti, J.G., 2000. **Regulation of actin filaments assembly by Arp2/3 complex and formins.** Development 127: 755-767.

Shelton, C.A., Carter, J.C., Ellis, G.C. and Bowerman, B., 1999. **The nonmuscle myosin regulatory light chain gene *mlc-4* is required for cytokinesis, anterior-posterior polarity, and body morphology during *Caenorhabditis elegans* embryogenesis.** J Cell Biol 146: 439-451.

Solon, J., Kaya-Copur, A., Colombelli, J., Brunner, D., 2009. **Pulsed forces timed by a ratchet-like mechanism drive directed tissue movement during dorsal closure.** Cell 137: 1331-1342.

Soto, M.C., Qadota, H., Kasuya, K., Inoue, M., Tsuboi, D., Mello, C.C., et al., 2002. **The GEX-2 and GEX-3 proteins are required for tissue morphogenesis and cell migrations in *C. elegans*.** Genes Dev 16: 620-632.

Sulston, J.E., Schierenberg, E., White, J.G. and Thomson, J.N., 1983. **The embryonic cell lineage of the nematode *Caenorhabditis elegans*.** Dev Biol 100: 64-119.

Vanneste, C.A., Pruyne, D., Mains, P.E., 2013. **The role of the formin gene *fhod-1* in *C. elegans* embryonic morphogenesis.** Worm: e25040

Vicente-Manzanares, M., Ma, X., Adelstein, R.S. and Horwitz A.R., 2009. **Non-muscle myosin II takes centre stage in cell adhesion and migration.** Nat Rev Mol Cell Biol 10: 778-790.

Walck-Shannon, E., Reiner, D., and Hardin, J., 2015. **Polarized Rac-dependent protrusions drive epithelial intercalation in the embryonic epidermis of *C. elegans*.** Development 142: 3549-3560.

Wang, J., Chitturi, J., Ge, Q., Laskova, V., Wang, W., Li, Z., Ding, M., Zhen, M., Huang, X., 2015. **The *C. elegans* COE transcription factor UNC-3 activates lineage-specific apoptosis and affects neurite growth in the RID lineage.** Development 142: 1447-1457.

Wernike, D., van Oostende, C., Piekny, A., 2014. **Visualizing neuroblast cytokinesis during *C. elegans* embryogenesis.** J Vis Exp 85: e51188.

Wightman, B., Ebert, B., Carmean, N., Weber, K., Clever, S., 2005. **The *C. elegans* nuclear receptor gene *fax-1* and homeobox gene *unc-42* coordinate interneuron identity by regulating the expression of glutamate receptor subunits and other neuron-specific genes.** Dev Biol 287: 74-85.

Williams-Masson, E.M., Malik, A.N. and Hardin, J., 1997. **An actin-mediated two-step mechanism is required for ventral enclosure of the *C. elegans* hypodermis.** Development 124: 2889-2901.

Wissmann, A., Ingles, J., McGhee, J.D. and Mains, P.E., 1997. ***Caenorhabditis elegans* LET-502 is related to Rho-binding kinases and human myotonic dystrophy kinase and interacts genetically with a homolog of the regulatory subunit of smooth muscle myosin phosphatase to affect cell shape.** Genes Dev 11: 409-422.

Wissmann, A., Ingles, J. and Mains, P.E., 1999. **The *Caenorhabditis elegans mel-11* myosin phosphatase regulatory subunit affects tissue contraction in the somatic gonad and the embryonic epidermis and genetically interacts with the Rac signaling pathway.** Dev Biol 209: 111-127.

Yamashiro, S., Totsukawa, G., Yamakita, Y., Sasaki, Y., Madaule, P., Ishizaki, T., et al., 2003. **Citronkinase, a Rho-dependent kinase, induces di-phosphorylation of regulatory light chain of myosin II.** Mol Biol Cell 14: 1745-1756.

Zhang, H., Gally, C. and Labouesse, M., 2010. **Tissue morphogenesis: how multiple cells cooperate to generate a tissue.** Curr Opin Cell Biol 22: 575-582.